Repair of Clustered DNA Lesions in Double Strand Break Repair Deficient Human Tumor Cells

by Charles William Loftin Jr.

March, 2010

Chair: Jeff McKinnon

Major Department: Biology

DNA-dependent protein kinase (DNA-PK) is a holoenzyme of three subunits, Ku70, Ku80, and the DNA-Pk catalytic subunit (DNA-PKcs). DNA-PK serves a role in non-homologous end joining to repair double stranded breaks, and has a suggested role in the expression of base excision repair (BER) proteins. Repair of DNA damage is vital to the prevention of malignant mutations. Oxidative induced clustered DNA lesions (OCDLs) is the occurrence of two or more closely located DNA lesions, and have been shown to be poorly repaired. DNA-PKcs is the phosphorylating unit of DNA-PK. DNA-PKcs deficient cells show increased radiosensitivity and decreased reparability. This study aimed to evaluate the role of DNA-PK in OCDL repair in DNA-PKcs deficient cells. This study showed decreased OCDL repair and a decreased expression of the BER protein XRCC1 in cells treated with DNA-PKcs specific inhibitors compared to non-treated cells. This study proposes that DNA-PK is involved in response to single and complex damage, and that inhibition of DNA-PKcs results in poor OCDL repair. Interest is growing in protein kinase inhibitors as supplemental aids to chemo and radiotherapies. This study and others indicates that DNA-PK is important to proficient DNA repair, indicating that DNA-PKcs inhibitors may have clinical relevance as supplemental aids to current cancer therapies in killing targeted cells.

Repair of Clustered DNA Lesions in Double Strand Break Repair Deficient Human Tumor Cells

A Thesis Presented To the Faculty

of the Department of Biology East Carolina

University

In Partial Fulfillment of the

Requirements for the Degree Masters

of Biology

by

Charles William Loftin Jr.

March, 2010

Repair of Clustered DNA Lesions in Double Strand Break Repair Deficient Human Tumor Cells

REPAIR OF CLUSTERED DNA LESIONS IN DOUBLE STRAND BREAK REPAIR

DEFIECIENT HUMAN TUMOR CELLS

by

Charles William Loftin Jr.

APPROVED BY:

DIRECTOR OF DISERTAION/THESIS:

_____

Alexandros Georgakilas, Ph.D.

COMMITTEE MEMBER:

_____

Colin Burns, Ph.D.

COMMITTEE MEMBER:

_____

Mary Farwell, Ph.D.

COMMITTEE MEMBER:

_____

John Stiller, Ph.D.

CHAIR OF THE DEPARTMENT OF BIOLOGY:

_____

Jeff McKinnon, Ph.D.

DEAN OF THE GRADUATE SCHOOL:

_____

Paul J. Gemperline, Ph.D.

ACKNOLEDGMENTS

TABLE OF CONTENTS

LIST OF FIGURES and LEGENDS

LISTS OF TABLES and LEGENDS

LIST OF ABBREVIATIONS

AP: Abasic site

BER: Base excision repair

CCD: Charge coupling device

CHEF: Clamped homogenous electric field

DMSO: Dimethyl sulfoxide

DNA-PK: DNA dependant protein kinase

DNA-PKcs: DNA dependant protein kinase catalytic subunit

DSB: Double strand break

DTT: DL-Dithiothreitol

EDTA: Ethylenediaminetetraacetic acid

EndoIII: Endonuclease III

FBS: Fetal bovine serum

HR: Homogenous recombination

LMDS: Locally multiple damaged sites

NALA: Number average length analysis

NER: Nucleotide excision repair

NHEJ: Non-homologous end joining

OCDL: Oxidative clustered DNA lesion

PBS: Phosphate buffered Saline

PFGE: Pulsed field gel electrophoresis

PVDF: Polyvinylidien diflouride

ROS: Reactive oxygen species

SCGE: Single cell gel electrophoresis

SDS PAGE: Discontinuous sodium dodecyl sulfate polyacrillamide gel electrophoresis

SSB: Single strand break

TBST: Tris buffered saline with tween

TM: Tail moment

XRCC1: X-Ray cross-complementing

INTRODUCTION AND BACKGROUND

Cancer and DNA Damage

Despite declining cancer mortality rates in recent years, it has been estimated that last year half a million people in the United States died of cancer (Jemal 2009). Environmental and intracellular factors contribute to genomic damage. When un-repaired this damage can lead to the development of cancer (Weinberg 1996). Cells follow a controlled pattern of genesis, propagation, and death. Gene mutations, specifically mutations in tumor suppressors and protooncogenes can result in cells inability to properly control their cell cycle and proliferation. The outcome of this uncontrolled cellular proliferation is tumorogenesis. Whether hereditary or occurring later in life, mutations in certain genes make cells more susceptible to becoming cancerous (Weinberg 1996).

The ability of a cell to prevent mutagenesis and potential carcinogenesis is predicated on its efficiency to repair DNA damage. Damage caused by oxidative agents and the cell's ability to repair this damage has been shown to be a contributing factor in cancer development (Kastan 2004). Oxidative stressors can arise from internal and external sources. As a consequence of internal metabolic processes oxidizing threats can occur as byproducts in the form of reactive oxygen species (ROS) (Neilson and Kroken 2001, Cadet 1998, and Cook 2003). Damage by external factors includes chemical carcinogens such as alkylating agents and ionizing radiation which produces strand breaks and creates ROS as well (Lindahl and Wood 1999 and Burma 2006, Miller 1978). These ROS, particularly the hydroxyl radical, have the ability to oxidize

DNA. The addition of an OH group to pyrimidine and/or purine bases results in improper

molecular base structures, which can cause bond breaks resulting in strand breaks (Cadet 1998,

and Cook 2003).

 As a result of the effects of ionization and oxidation, DNA damage can be presented in the

forms of (seen below in Figure 1) single and double stranded breaks (SSBs and DSBs), abasic

sites, and oxidized bases (Ward 1994 and Georgakilas 2008). These types of damage are

proficiently repaired, but not when closely grouped (Ward 1981 and Goodheade 1994). The

observation of disproportionately high cytotoxicity compared to the amount of DSB damage

following ionizing radiation prompted Ward to theorize the concept of locally multiple damaged

sites (LMDS). This concept linked poor repairability to the closeness of DNA damage sites

(Ward 1981). Clustered DNA lesions can be presented as DSBs or non-DSB oxidative clustered

DNA lesions (OCDLs). Studies have shown OCDLs to have poor repairability (Georgakilas

2004). OCDL's as the name suggests, are lesions that appear clustered closely together, within

10 base pairs of one another (Sutherland 2000, Francisco 2007, Gollapalle 2007). Examples of

DNA damage can be see below.

Figure1. Non-Clustered Damage

Simple DNA Damage

Oxidized Base   Abasic Site

Single Strand Break   Double Strand Break

Clustered DNA Lesion

Complex Base Damage   Complex DSB   Complex SSB
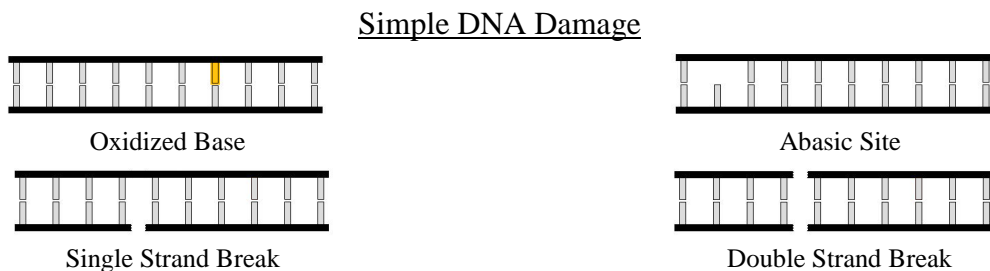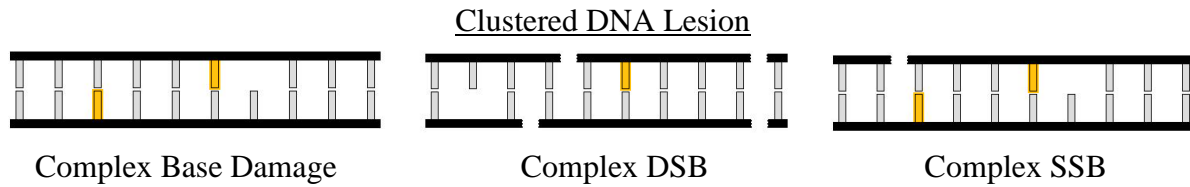
Figure 2. Clustered DNA Lesions

DNA Repair

DNA damage repair is performed by various pathways. SSBs, oxidized bases and abasic sites are repaired through base excision repair abbreviated BER, or by nucleotide excision repair, abbreviated NER (Cook 2003 and Georgakilas 2008). Damage caused as previously described, by low level ionization and endogenous factors are believed to be primarily repaired by BER (Lindahl and Wood 1999). As seen below, BER utilizes DNA glycosylase to create an abasic site by indentifying and excising a damaged base. AP-endonuclease then cleaves at the abasic location creating a break in the strand. Following this, DNA polymerase is able to reinstate a new corrected nucleotide at the site. DNA ligase then seals the strand (Georgakilas 2008, and Hada and Georgakilas 2008).

Figure 3. Base Excision Repair Pathway

Of greater mutagenic concern than SSBs is the occurrence of lesions that occur parallel along the helix, producing double strand breaks. DSBs are considered more complex to repair, and therefore their occurrence is more of a threat to genomic stability (Jackson 2002). Double strand breaks, depending on the phase of the cell cycle are believed to be repaired by either homologous repair (HR) or non-homologous end joining (NHEJ) pathways (Burma 2006 and Peddi 2008). OCDL's may pose still a greater threat. OCDL's have been shown to be poorly repaired, if repaired at all, thereby eliciting increased mutagenic potential (Georgakilas 2008). Additionally, as reviewed by Georgakilas, some studies suggest that glycosylase and endonuclease excising activities may be compromised in clustered lesion repair (Georgakilas 2008).

Detection of DNA Damage

The use of single cell gel electrophoresis (SCGE or Comet Assay), and pulsed field gel electrophoresis (PFGE) have been used for studying the processing of OCDLs by detection and measurement of SSBs and DSBs respectively. Glycosylases and endonucleases are used in the BER pathway to induce a strand break where a corrected base can be inserted. Based on that concept, bacterial DNA repair enzymes can be used to create strand breaks at oxidized base sites, enabling the detection and measurement of those oxidized bases (Sutherland 2000, Hada and Georgakilas 2008). EndonucleaseIII repair enzymes (EndoIII) uses glycosylase activity to remove oxidatively damaged pyrimidines (Saito 1997). Like EndoIII, Fpg repair enzymes use glycosylase activity, but to remove damaged purines (O'Conner 1992). See Table 1 for a full list of base damages cleaved by Fpg and EndoIII. Excision of bases by these enzymes creates an abasic (AP) site that marks the incision point for the enzyme's abasic lyase activity to form a

4

SSB. Simultaneous cleavage of cluster lesions on closely located opposing strands results in

forming DSBs (Sutherland 2000). As seen in the depiction below, the increase in detected

breaks created by the repair enzymes at oxidized bases indicates the amount of OCDL damage

(Sutherland 2000).

Figure 4. Detection of Clustered DNA Lesions

Clustered DNA Damage

AP site or oxidized base

I

Enzyme treatment   II   **AP site oxidized base**

Neutral agarose gel

No strand break   Detection of clusters   **DSB**

SSB

No detection of clusters

Radiation: -   +
Enzyme   -   +   -   +

OCDL
DSBs
OCDL

1   2   3   4
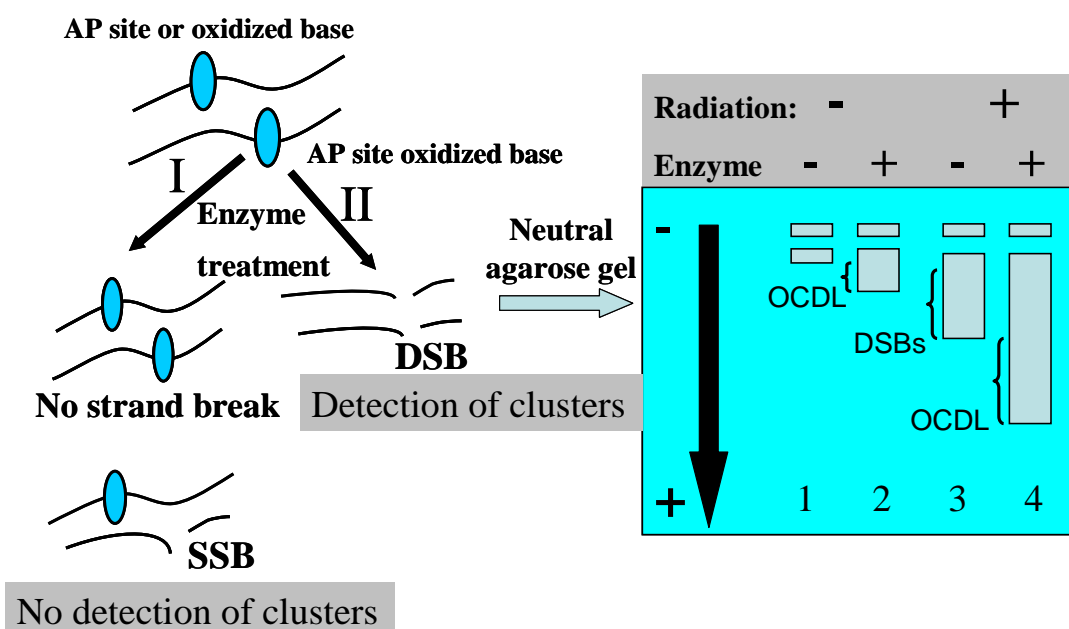
(Hada, and Georgakilas 2008) Detection of clustered DNA lesions (double strand breaks, DSBs and oxidative clustered DNA lesions, OCDL). (A) Principles of detection using a repair enzyme for a representative type of a cluster consisting of a set bistranded base lesions as originally introduced by Sutherland (Sutherland 2000). Alternatively one of the lesions can be a single strand break, SSB. As shown in pathway I, incomplete cleavage of both lesions by the repair enzyme will lead to no detection of the cluster. In the case of cleavage of both lesions by the enzyme and induction of a DSB, detection of the cluster occurs. (B) Detection of clusters using neutral agarose gel electrophoresis. Genomic DNA (T7 or λ) or human DNA can be subjected to agarose gel electrophoresis (constant or pulsed field) and with application of number average length analysis (NALA) the DSBs and OCDL can be measured in the same gel as the additional to the ones being induced by radiation. For lanes 1,2 (non-irradiated) low levels of endogenous OCDL are expected. For lanes 3,4 (irradiated) higher levels of OCDL are expected. Comparison of lane 3 and 1 will provide the yield of prompt DSBs. **(Provided courtesy of A.G. Georgakilas)**

Detection and measurement of SSBs and oxidized base damage was done using a novel alkaline (denaturing) adaptation of the comet assay based on a previous method using DNA agarose plugs as in PFGE (Visvardis 2000). The comet assay, also known as single cell gel electrophoresis (SCGE) or micro-gel electrophoresis, can be performed using alkaline or neutral conditions for the detection of SSBs (alkaline), DSBs (neutral), and oxidized bases (Hada and Georgakilas 2008). As reviewed by Fairbairn et al., the alkaline comet assay uses electrophoresis to force migration of fractured DNA by its negative ends through a gel medium. This is done under alkaline conditions to allow the unwinding and denaturation of DNA. During electrophoresis the fragmented DNA migrates forming a tail (Fairbairn 1995). This tail (as seen below) behind the cell is much like what is seen in a comet, hence the name. The tail moment (TM) of this cell is proportional to the amount of damage (see below). Oxidative damage was induced by using hydrogen peroxide, which has shown to induce only SSBs primarily, making it a suitable substitute for γ-irradiation in the study of SSB repair (Djuric 1993, and Holt and Georgakilas 2007). There appears to be modest research into the use of repair enzymes with comet assay to detect non-DSB clusters. The inability of repair enzymes to cleave all damaged sites can result in clusters not being detected (Hada and Georgakilas 2008). However, alkaline electrophoresis can produce breaks at any site that is alkali labile allowing for the detection of existing SSBs. These alkaline conditions can cause strand break formation at oxidized bases sites, such as 5,6-dihydroxy-5,6-dihydrothymine, 5-formyluracil, oxazolone, and in oxidized abasic sites (Pouget 2002, Douki 2006).
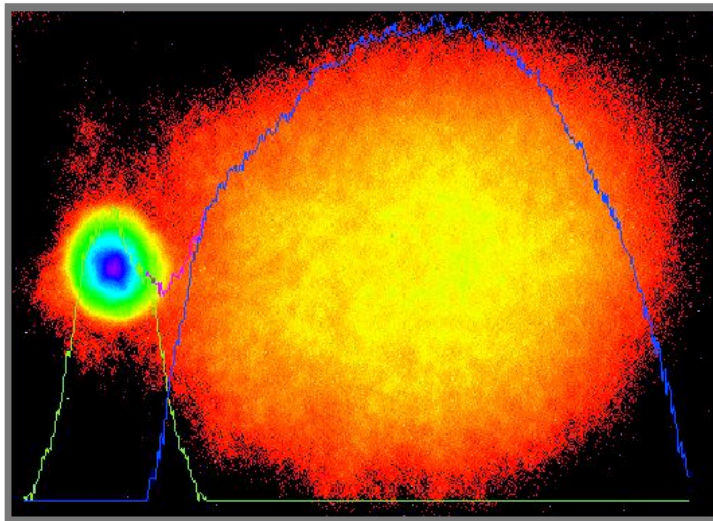
Figure 5. Computer screenshot of a scored comet
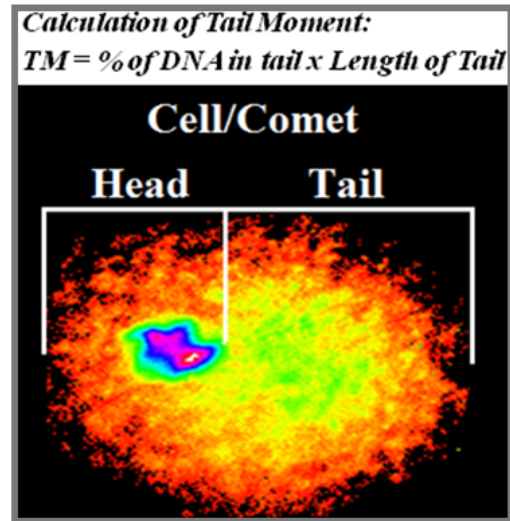
Figure 6. Alkaline Comet assay picture and tail moment formula

Pulsed field gel electrophoresis was used for the first time in the early 1980's as a solution to unsuccessful attempts to separate out large DNA molecules (Schwartz and Cantor 1984). DSBs were shown to be measurable by PFGE using the clamped homogenous electric field (CHEF) technique. CHEF uses electrophoresis at different angles surrounding a gel to force migration of small to large DNA fragments up to 10Mbp through a gel (Blöcher 1989). Two or more strand breaks occurring within 20 base pairs of one another on opposite strands produce a DSB (Sutherland 1999). PFGE or CHEF has been an effective method for the measurement of DSB damage and repair. However, until nearly a decade ago no method existed to quantify the amount of clustered damage in large DNA fragments. Sutherland et al., devised a method using repair enzymes as damage probes that cleave DNA at oxidized purines and pyrimidines creating SSBs at oxidized and abasic sites. When SSBs form in close proximity on opposing strands this forms DSBs that can be measured using PFGE. Using repair enzymes additional SSBs are

7

created thereby creating additional DSBs. These DSBs are additional to the ones induced directly by the oxidizing agent and are equal to the number of clusters existing (Sutherland 1999). PFGE quantification of OCDL repair following low level γ-irradiation used treated and non-treated repair enzyme agarose plugs with isolated DNA. The DNA within these plugs was cleaved using restriction enzymes. The plugs were then loaded into individual wells/lanes and assayed using CHEF conditions. The samples were electrophoresed through a gel medium alongside lanes containing standardized lengths of DNA within the expected migration boundaries of the samples. The migrations of these samples provide the data needed to create a dispersion curve comparing DNA length with migration. A charge coupling device (CCD) camera is used to fluoresce and photograph DNA. The calculations used account for the amount of DNA present. Therefore, gels were stained using ethidium bromide so the DNA fluoresced equaled the amount of DNA present in each sample lane (Sutherland et al. 2003). The Software Quantiscan (BioSoft, Cambridge, UK) allows the amount of fluoresced DNA to be quantified. Using computer software in conjunction with the dispersion curve data from the DNA length markers, a densitogram is made for each sample lane in the PFGE gel (see below) and used to calculate the number average length analysis or NALA (Ln). NALA calculations as seen below (Equation 1) were made for each sample comparing florescence of DNA and migration. The number of DSBs for irradiated samples was found by comparing the number average length difference for the irradiated and non-irradiated samples (Equation 2). Similarly, the detection and measurement of oxidized bases was calculated using the Ln differences of radiated samples with and without repair enzyme treatment (Equation 3) (Sutherland 2000).

Number Average Length Analysis (NALA) used in the calculations of DSBs and OCDLs

(Equation 1) NALA: $Ln = [\int f(x) \ dx \ ] / [\int f(x) / L(x)]$

(Equation 2) DSB Frequency $= 1/Ln(Radiated) -1/Ln(Non\text{-}Radiated)$

(Equation 3) OCDLs Frequency $= 1/Ln(Radiated+Enzyme) -1/Ln(Radiated\text{-}Enzyme)$

Ln=Number average lenth, L(x)=migration distance, f(x)dx=fluorescence   (Sutherland 2000)
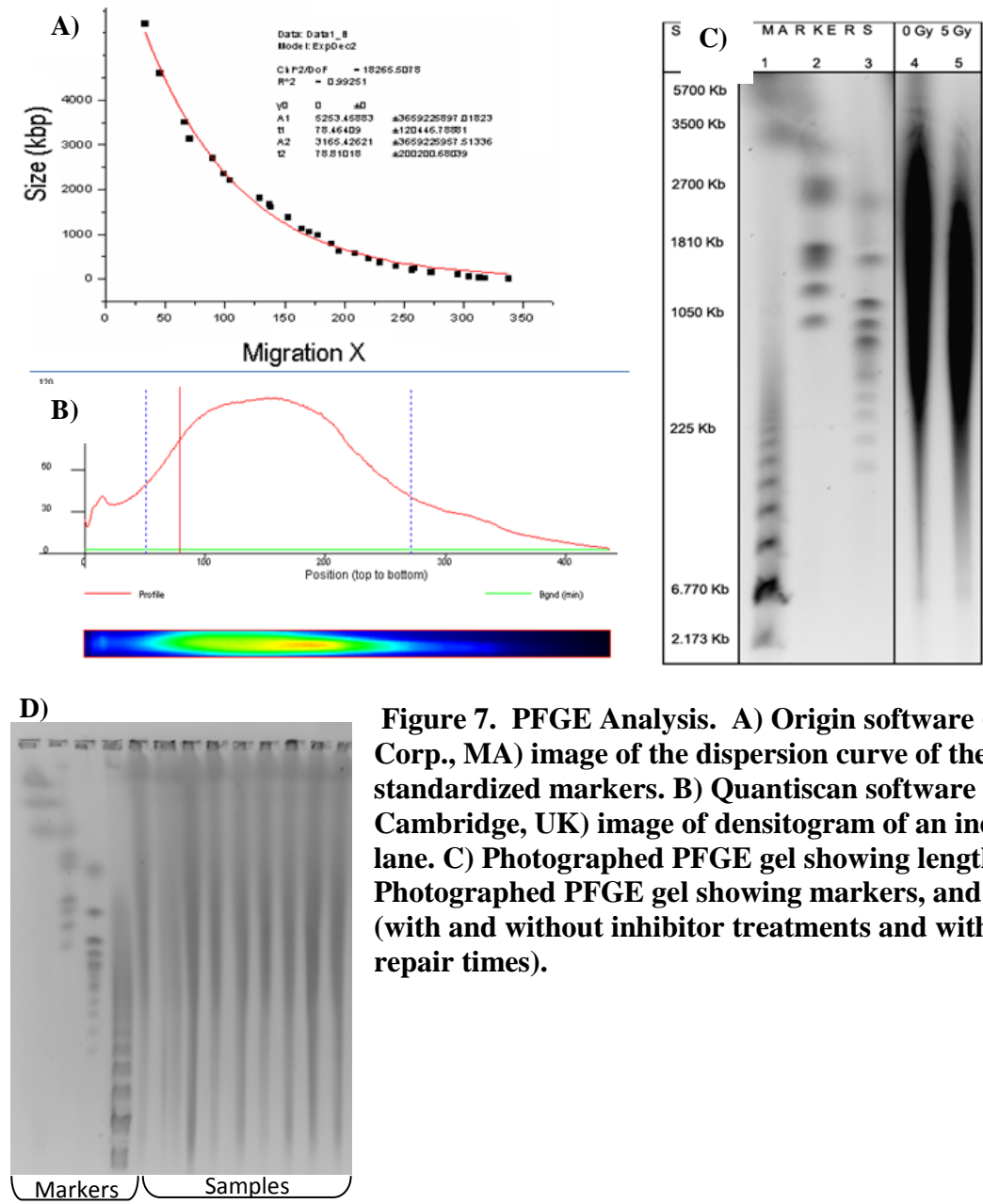
Figure 7. PFGE Analysis. A) Origin software (OriginLab Corp., MA) image of the dispersion curve of the PFGE standardized markers. B) Quantiscan software (BioSoft, Cambridge, UK) image of densitogram of an individual PFGE lane. C) Photographed PFGE gel showing length markers. D) Photographed PFGE gel showing markers, and sample lanes (with and without inhibitor treatments and with differing repair times).

DNA-PK and DNA Repair

DNA Dependent Protein Kinase, abbreviated DNA-PK is a holoenzyme of three subunits, Ku70, Ku80, and DNA-Pk catalytic subunit (DNA-PKcs). DNA-PKcs is part of the phospatidylinositol-3-kinases (Smith and Jackson 1999). The Ku portions of DNA-PK are named Ku70 and Ku80 corresponding to their kilodalton weight (Chan 1996). It is believed that the Ku heterodimer detects and attaches to the ends of double strand break sites. To damaged sites, the Ku proteins recruit DNA-PKcs which is believed to help orchestrate the non-homologous end joining (NHEJ) process by its activation of repair proteins via phosphorylation (Smith and Jackson 1999, Kashishian 2003, and Hudson 2005). Studies also show repair by homologous recombination (HR) is decreased when DNA-PKcs expression is inhibited. Thereby, suggesting a possible link of DNA-PKcs in the proper induction of HR (Allen 2003).

Evidence from this study and others suggests the importance of DNA-PKcs to DSB repair, showing increased ionizing radiation sensitivity and decreased repair in cells not expressing DNA-PKcs and in DNA-PKcs inhibited cells (Kashishian 2003). Aside from the induction of the repair pathways, DNA-PK has been shown to be linked to cells' ability to overcome G2 cell cycle arrest (Arlander 2008). Following damage, the cell cycle may be arrested at checkpoints. Normally damage is repaired and the arrest is overcome. However, in DNA-PK inhibited or mutated cells this arrest is much more prolonged and thereby results in higher levels of cell death (Arlander 2008).

Strand breaks are believed to interfere with the repair of nearby base lesions, thereby making clustered lesions difficult to repair (Dianov 2001). SSBs and non-DSB OCDLs are believed to be mainly repaired by the BER pathway (Peddi 2008). DNA-PK expression is thought to be involved in BER protein activation (Levy 2006, and Parlanti 2007). One of these BER proteins shown to have association with DNA-PK is XRCC1 (Levy 2006). Studies indicate that in response to oxidative stress, XRCC1 is stabilized/activated by DNA-PKcs phosphorylation (Toulany 2008). X-ray cross-complementing or XRCC1 is a base excision repair protein shown to aid in decreasing radio-sensitivity and SSB repair, and is believed to function as a scaffolding protein (Thompson 1990, and Mourgues 2007). Inhibition of DNA-PKcs expression therefore, could impede the expression of BER proteins such as XRCC1.

DNA-PKcs Inhibitors

Two drugs were used in this study to inhibit DNA-PKcs. The primary drug used was 1-(2-hydroxy-4morpholin-4-yl-phenyl)-ethanone which is called IC86621. Created by the Washington based ICOS Corporation, IC86621 is an effective inhibitor of proteins in the phoshatidylinositol-3-kinase family, which DNA-PKcs is a member of. IC86621 has little effect on related members of the phosphotidyl inositol kinase family such as ATM and ATR. Biochemical and genetic studies of IC86621 have demonstrated its function as a specific inhibitor of DNA-PK kinase activity (Allen 2003, and Kashishian 2003). When used in combination with certain chemotherapeutic agents such as bleomycin there has been evidence of increased tumor cell death (Baily 2003, and Kashishian 2003). To corroborate that results were due to DNA-Pkcs inhibition and not an unidentified supplemental feature of the IC86621, effects

of another novel DNA-PKcs specific inhibitor (2-(morpholon-4-yl)-benzo[h]chomen-4-one) or NU7026 was tested as well (Veuger 2003 and Wilmore 2004).

Cells Studied

 MCF-7 cells are cancerous breast cells, and are DNA-Pkcs proficient. These cells are regularly used in breast cancer studies. The original cells of this line were taken from breast cancer patient at the Michigan Cancer Foundation in the early 1970's (Nugoli 2003). MO59J and MO59K cells are also cancerous cells. Both MO59J and MO59K are isogenic human glioblastoma cells that were taken from different areas of the same biopsy. MO59K express DNA-PKcs, whereas MO59J cells are deficient for DNA-PKcs (Lees-Miller 1995, and Dibiase 2000).   Glioblastomas and breast cancer cells were suitable for this study because of the epidemiological significance of these cancers as well as the unique difference in DNA-PKcs expression of the MO59K and MO59J cells. Glioblastomas are considered one of the most deadly forms of cancer, and unfortunately are also the most common form of central nervous system malignancies (Parsons 2008, and Stupp 2005). While treatable with surgical removal, chemotherapy and radiotherapy, the survival outlook for a majority of patients does not extend past one year following tumor discovery (Stupp 2005). Due to advantages in treatment and early detection three quarters of those diagnosed with breast cancer now survive (Jemal 2009). However, its rate of incidence is high. Breast cancer is the most prevalent form of cancer in women worldwide. In a 2002 statistical study female breast cancer accounted for 31.3% of documented incidences of cancer in North America, and 23% worldwide (Parkin 2002).

HYPOTHESIS

Various studies suggest multiple roles for DNA-PK not only in the repair of DSBs, but also other oxidatively-induced DNA lesions (reviewed in Georgakilas 2008). Initial experiments using the cell line MCF-7 indicated that the drug IC86621 was efficient at suppressing base excision repair, resulting in overall deficient processing of lesions such as SSBs. Initial experiments utilizing MCF-7 cells also showed reduced expression of the repair protein XRCC1 following IC86621 treatment. By inducing and analyzing single strand breaks, double strand breaks, abasic sites and oxidized bases in DNA-PKcs deficient and proficient malignant cell lines this study aims to identify the role of DNA-PKcs in OCDL repair. It is hypothesized that the chemical inhibition of the activity of the catalytic subunit of DNA-PK will result in compromised clustered lesion processing, and reduced expression of the BER protein XRCC1.

OBJECTIVES

The primary objective of this study was to evaluate the role of DNA-PK in the processing of

oxidative clustered DNA lesions in cells with proficient and deficient DNA-PKcs repair

pathway. MO59K human glioblastoma cells and MCF7 human breast cancer cells express

DNA-PKcs. To examine the role of DNA-PK in processing of clustered DNA damage, its

kinase activity was chemically inactivated using novel inhibitors IC86621 and NU7026 in MCF7

and MO59K cells. DNA-PKcs deficient MO59J otherwise isogenic to MO59K served as a

control.   Damage and repair was measured using alkaline comet assay, and pulsed field gel

electrophoresis (PFGE). DNA-PK is postulated to have a role in BER deficiency (Levy 2006,

and Toulany 2008). Immunobloting was used to discern the effect DNA-PKcs expression had on

the expression of BER protein XRCC1 post oxidative stress.

Specific Objectives:

1. DNA-PKcs deficiencies are thought to compromise repair of single oxidativly-induced

clustered DNA lesions. Alkaline comet assay methods probe for SSBs. H_2O_2 was used to

induce single oxidative DNA lesions (Holt and Georgakilas 2007). Comet assays using repair

enzymes allowed for repair analysis of SSBs, oxidized bases, and abasic sites in DNA-PKcs

deficient MO59J cells and in DNA-PKcs inhibited and non-inhibited MO59K and MCF7 cells.

2. DNA-PKcs has been shown to function in NHEJ pathway in DSB repair. PFGE assays with

NALA analysis were used to compare the repair of DSB and non-DSB OCDLs. This PFGE

repair study used DNA-PKcs deficient MO59J cells and in DNA-PKcs inhibited and non-inhibited MO59K and MCF7 cells at incremental time points following low level γ-irradiation.

3. Western blotting was used in non-treated and drug treated MO59K, MO59J, and MCF7 cells to analyze the expression levels of the BER protein XRCC1 and it relation to the expression of DNA-PKcs following oxidative damage.

SIGNIFICANCE OF WORK

Various risk factors associated with cancer such as heredity, environmental conditions, and life style has been recognized. Over the last years much has been learned about cancer etiology. Contributions of particular note include the delineation of the role of DNA repair factors to cancer risk, and especially the discovery and quantification of risks associated with gene mutations in DSB repair factors. This work is original and targets for the first time the important role of DNA-PKcs in the processing of oxidatively induced clustered DNA damage in several human cancer cell lines.

Although significant knowledge exists about DNA-PKcs function in the processing of double strand breaks, there is no knowledge currently of the effect of a compromised DNA-PKcs pathway in the processing of oxidatively-induced complex DNA damage. Our results provide evidence for a role of DNA-PKcs in the processing of different types of oxidative DNA lesions and suggest different mechanisms by which this effect is exerted. The information rendered by this novel study will be important not only for understating cancer etiology in the presence of a NHEJ deficiency but also lead to a better understanding of cancer treatments based on the inhibition of DSB repair

METHODOLOGY

Cell Culture

Three cell lines, MO59K, MO59J, and MCF-7 have been used. MCF-7 malignant breast epithelial cells were acquired from the company ATCC. The MCF-7 cells were grown in RPMI 1640 medium. RPMI 1640 media was attained from Gibco and contained 1 mM sodium pyruvate, 2 mM L-glutamine, 4500 mg/L glucose, 10mM HEPES, and 15 mg/L sodium bicarbonate. In addition to the existing components, the total volume of the media was complemented with 10% fetal bovine serum or FBS (Invitrogen), 0.1% human insulin (Gibco). Cells were grown in either 25 cm^2 or 75 cm^2 flasks in an incubator maintaining 37˚C and a 5% CO_2 environment.

MO59K and MO59J cells were also purchased from ATCC. The MO59J and MO59K cells were grown in 50:50 DMEM / F-12 (1X) with L-glutamine medium acquired from Cellgro. DMEM / F-12 medium was complemented with 10% fetal bovine serum and 1% MEM Non-Essential Amino Acid Solution 10mM (100X) both acquired from Intvitrogen. Like the MCF-7 cells the MO59J and MO59K cells were grown in 25 cm^2 or 75cm^2 flasks in an incubator maintaining 37˚C and a 5% CO_2 environment. Cells were allowed to grow to between 75-85% confluency before being split. Cell medium was changed generally every 4 days.

Alkaline Comet Assay

Alkaline comet assays were performed using MO59K, MO59J and MCF7 cells acquired from 0, 3, and 12 hour repair time points. Each time point had three associated conditions, the conditions were (no H_2O_2 /with no IC86621) as the control, (no H_2O_2/with IC86621), and (H_2O_2 treated/with IC86621). The MO59J cells were also be used and had the same time points and conditions with the exception of the drug treatment. Comet assays performed for each cell line, MCF-7, MO59K and MO59J each followed the same protocol. Stock solutions of 50 mM IC86621 (Sigma) dissolved in dimethyl sulfoxide (DMSO) was made prior to culturing the cells and stored in the dark at -20˚C. Cells were grown in 25 cm^2 flasks.

Once 75% confluency was reached aliquots of IC86621 in DMSO were thawed and were placed into the cell medium (DMEM/ F-12 for the MO59 cells and RPMI for the MCF7 cells) giving the medium an IC86621 concentration of 100 µM. DMSO was then placed into the control cell flasks. The control cells and the drug treated cells both have a final DMSO concentration of 0.2%. The cells were then allowed to incubate with the drug at 37˚C for 24 hours to allow time for the drug to uptake and begin inhibiting the expression of DNA-PKcs. Following incubation the designated drug treated cells were treated with 100 µM H_2O_2 on ice for 20 minutes (Holt and Georgakilas 2007, Peddi 2008). Following the hydrogen peroxide treatment the 0 hour repair time cells were then detached from their flask using 2X Trypsin with EDTA (Trypsinization), and a cell count was performed. The agarose plugs made in the comet assays contained 10,000

cells a piece. Therefore, the cell counts taken were used to determine the number of plugs that were able to be made.

The cells were next centrifuged, and washed with 1X phosphate buffered saline solution (PBS). A 50-50% solution of TE (10 mM tris-HCl, 1 mM EDTA, pH 7.5) and 1.6% low melt agarose was made. Each plug consisted of 100 µl of this half TE half 1.6% low melt agarose solution. Therefore, the total number of cells determined how much of this solution was needed to suspend the pellet. (i.e. the more cells one had, the greater amount of TE/low melt agarose solution). The cell pellet was suspended in the appropriate amount TE/agarose solution, then pipetted into plastic plug molds. The plug molds were next placed in a 4°C environment and allowed to solidify. Once the plugs were formed they were stored at 4°C in a pH 7.5 TE solution that had been argonated and supplemented with 50µM PBN to prevent free radicals. Cells from the 3 and 12 hours repair times were allowed to incubate at 37°C in fresh medium containing either 100 µM of IC86621 in DMSO or an equivalent volume of DMSO only (non-inhibited samples) for their respective conditions and repair times (Peddi 2008). At the conclusion of their specific repair times these cells were then processed into comet assay plugs in the exact same fashion as described above for the 0 hour repair time cells.

Following plug production cells encased in the plugs were lysed using a solution of 10% DMSO, 1% Triton X100, and 89% Lysis solution (10 mM Tris, 100 mM EDTA, 2.5 M NaCL, pH 10.00). Plugs were then placed into the solution to lyse for two hours. Assays were also preformed to detect Fpg or EndoIII enzyme cleavage sites, for these assays additional steps were

followed next. For EndoIII, and Fpg treatments the plugs were next treated with two 30 minute

treatments using an enzyme buffer specific for each enzyme (EndoIII buffer: 20 mM Tris-HCl, 1

mM EDTA, pH=8.00) (Fpg buffer: 10 mM Tris-HCl, 10 mM $MgCl_2$, pH 7.00) at 4ºC. Plugs

were placed in a solution consisting of 1% 100X DTT, 1% Enzyme (either EndoIII of Fpg at

0.25 units/uL both purchased from New England Biolabs), and 98% Enzyme buffer (same as

aforementioned enzyme buffers). The plugs were then incubated in this solution for one hour at

4˚C then another hour at 37˚C.

Next, standard plugs and enzyme treated plugs both were placed into electrophoresis buffer (300

mM NaOH, 1 mM EDTA, pH 12.89) for 45 minutes, then fixed to agarose frosted glass

microscope slides using 0.8% low melt agarose solution in TE. Slides were placed at 4˚C for 15

minutes or until the plug is fixed to the slide. The slides were next placed into an electrophoresis

running apparatus in electrophoresis buffer and allowed to equilibrate for 15 minutes, and then

electrophoresed at 0.7 volts/cm and 300 mAmps for 30 minutes at 4˚C. Slides were next washed

in neutralizing solution (0.4 M Tris-HCl, pH7.5). The neutralizing step consisted of 3 separate

washes of 5, 5 and 15 minutes. To lessen drying time, slides were then placed in 70% ethanol

for 10 minutes then placed in a darkened room inside a ventilation hood. Plugs were allowed to

dry overnight.

So that cells would be visible under fluorescent light, plugs were stained with 10 µM of 1X

SybrGreen acquired from Canbrex Bioscience, and cells were photographed using an Olympus

BX40 fluorescent microscope with camera. Approximately 100 cells were photographed at 20X magnification. Analyzation of the cells single strand breaks as determined by tail moment was performed by uploading photographs into CometScore™ software program (Tritek Corp., VA). This program allowed the DNA damage and repair to be quantified and compared based off of the tail moment of the cells, which is the tail length multiplied by the percent of fluoresced DNA in tail.

Cell Lysis for Protein Lysates

Cell lysis procedures were done the same for each cell line. However, for MCF7 cells and for the MO59J and K cells different cell culture mediums were used. The difference in these conditions was previously described. Cells were detached using 2X Trypsin with EDTA, and fresh media was added to deactivate the trypsin. The contents of the flask were then be transferred into a 15 mL falcon tube and centrifuged at 2000 RPM for 5 minutes, forming a pellet. The supernatant was then poured off and the pellet was then re-suspended in 1 mL of fresh medium, and transferred into a 1.5 mL centrifuge tube. The tube was then centrifuged at 12RCF for 10 minutes, and then its supernatant was removed. The pellet was then washed with 1X phosphate buffered saline (PBS) and centrifuged for 5 minutes at 12RCF, this was done twice.

The supernatant was again be removed off the pellet and a lysis solution of 90 μL nuclear extraction buffer (2 mM EDTA, 10% sucrose, 50 mM Tris HCL, 1 mM DTT, 20% glycerol, 0.5 mM NaCl), 3 μL PMSF, and 7 μL protease inhibitor cocktail was placed into the centrifuge tube,

vortexed, and allowed to incubate on ice for 30 minutes (Peddi 2008, and Francisco 2008). The cells were then sonicated using 3 short bursts and then using a small scoopula, cells were mixed and crushed against the sides of the tube. Cells were then centrifuged again for 30 minutes at 12 RCF in a 4ºC cold room to prevent heat degradation of proteins (Peddi 2008, and Francisco 2008). Supernatant containing the cellular proteins was pipetted off and stored in a new centrifuge tube at -20˚C.

Western Blot

Prior to performing western blotting, the protein concentration of the cell lysates was found by performing a Bradford assay using standardized protein concentration kit (BioRad). Whole cell protein samples loaded into the gels will contain normally between 20-40 µg of protein, each sample in a respective gel always contained equal amounts of protein. Protein lysates were combined with 2X loading buffer (2.5% SDS, 5% beta-mercampoethanol) and boiled together for 10 minutes, and followed by one minute on ice before loading. The volume of lysate needed varied depending on their concentration. Discontinuous sodium dodecyl sulfate polyacrilimide gel electrophoresis (SDS PAGE) was carried out using 4-20% Tris-HCl precast gels (BioRad) and MiniProtean 3 cell electrophoresis device (BioRad). The molecular weight marker Kaleidoscope (BioRad) was loaded into un-used well in the gel. The electrophoresis was performed for 90 minutes at 180 volts and 70 mAmps at 4˚C. Following SDS PAGE, the proteins and their position with the gel was transferred to a Polyvinylidiene diflouride (PVDF) membrane (Millipore). PVDF membrane was cut in a size matching that of the gel, then activated by a 20 second washing in methanol, and then followed by a 2 minute wash in ddH$_2$O.

The membrane along with filter paper (BioRad), sponges, and gel were allowed to equilibrate in transfer buffer (25 mM Tris-base, 192 mM glycine, pH 8.3) for 15 minutes prior to the transfer process. These items were then clamped together and placed into a Mini-Trans Blot Cell transfer device (BioRad) and the transfer will be performed at 90 volts and 350 mAmps for 480 minutes at 4˚C.

The membrane was again soaked in 100% methanol and allowed to dry. The membrane was then be soaked in a blocking buffer of 5% non fat milk in 1X Tris buffered saline with tween (TBST) for one hour at room temperature, and briefly washed in TBST. The membrane was then incubated overnight on a slow rocker at 4ºC in solution of 2.5% non fat milk in TBST containing monoclonal mouse antibodies specific for XRCC1 (Abcam) at a 1000:1 ratio along and Beta-Actin antibody (Ambion) at a 3000:1 ratio. Membrane was then washed for one hour with TBST, and with 6 changes. The secondary antibody solution consisted of 100% TBST and the secondary goat anti-mouse antibody (Thermo Scientific) was placed in at a 500:1 ratio. The membrane was allowed to soak in the secondary antibody solution at room temperature for one hour under slight agitation, and was then washed as before for one hour in TBST. Equal amounts of SuperSignal West Dura stable peroxidase and luminal enhancer solution (Thermo Scientific) were mixed together and pipetted over the membrane. After five minute incubation at room temperature, the membrane was drained of any excess solution and sealed in plastic-wrap. Using a FlourChem^{TM} 8800 imaging system (Alpha Innotech, San Leandro, CA) an image was acquired.

Pulsed Field Gel Electrophoresis

Pulsed field gel electrophoresis (PFGE) like alkaline comet assay, required the creation of agarose plugs containing suspended cells. The production of these plugs was done in a similar fashion as previously described. The difference in the plug production was the number of cells used. For PFGE 200,000 cells were needed per plug to assure that an adequate amount of DNA was present in each sample (Tsao 2007, Peddi 2008, and Francisco 2008). Again DNA-PKcs inhibition was studied using inhibiting drugs on the MO59K and MCF7 cells. MO59K cells were treated with 100 µM of IC86621 in an identical fashion to the IC86621 treatments described in the comet assay section (Peddi 2008). However, for the MCF7 cells a different DNA-PKcs inhibitor was be used. MCF-7 cells were treated with 10 µM NU7026 (Sigma), both cell lines incubated at 37ºC and 5% CO_2 in their respective inhibitors for 24 hours prior to irradiation. Cells were transported on ice to the Brody school of Medicine. Using the Gammacell 40 (MDS Nordion, Kanata, Ontario, Canada) the cells were exposed to 5Gy of ^{137}Cs γ irradiation (Tsao 2007, Peddi 2008, and Francisco 2008). Post irradiation, 0.5 M EDTA was pipetted into initial (0 hr) sample flasks, and all flasks were placed back on ice. Flasks were placed back at 37ºC and 5% CO_2 conditions until their respective repair times were reached.

The production of multiple samples required many cells. Approximately two million cells were needed per flask so that multiple plugs could be made. After trypsinization, cells were counted and centrifuged at 2000 rpm's for 5 minutes to form a pellet. The pellet's supernatant was removed, and to cease any reactions again 0.5 M EDTA was pipetted onto the sample. The pellet was then suspended in 1.6% low melt agarose. The amount of agarose used was calculated

so that each plug made possessed 200,000 cells. Once suspended, the cells in low melt agarose

were pipetted into plug forming plastic molds and allowed to solidify at 4˚C. At this point the

plugs were stored at 4ºC in a storage buffer of argonated TE pH 9 and containing 50 µM PBN.

The plugs were next placed into 2 one hour soaks in fresh TE buffer pH 7.5. To lyse the cells

within the plug, the plugs were next placed into a PFGE lysing buffer (100 mM EDTA, 20mM

NaCl, 10 mM Tris-HCl, at pH 8.3) supplemented with 1.5% n-lauaroylsarcosine, and 2%

proteinase K for two hours on ice then the incubated at 37˚C for 24 hours. This was repeated for

each sample three times (Peddi 2008). Therefore, for 3 days the plugs were transferred into new

solution each day then re-incubated. After the three day lysing the lysing solution was removed

and the cells were washed for one hour with a solution of 40 mg/ml of phenylmethylsulfonyl

fluoride (PMSF) in NTE buffer (150 mM NaCl, 10 mM Tris-HCl, and 0.1 mM EDTA, at pH 8).

Next the NTE was removed and Asc-1 buffer (20 mM Tris-acetate, 10 mM magnesium acetate,

and 50 mM potassium acetate, at pH 7.9) was pipetted onto the plugs. The Asc-1 solution was

changed out every 20 minutes for an hour then the plugs were incubated at 4˚C for 24 hours in

the Asc-1 buffer. Each sample plugs were then placed into centrifuge tubes of 300 µL of fresh

Asc-1 buffer, and 3 µL of 100X DTT and 5 units ASC -1 enzyme. The tubes were then

incubated at 37˚ for 16 hours, after which 2 additional units of ASC-1 were added. Following

ASC-1 treatments, the plugs had three 20 minute washes in a stop solution of 70 mM Hepes-

KOH, 100 mM KCl, and 100 mM EDTA, at a pH of 7.6 (Peddi 2008). At this point the plugs

were ready to be either stored again or used for PFGE DSB analysis. However, for the plugs

used to test for enzyme repair sites, additional enzyme treatments were added.

For repair enzyme treatment plugs, the previous solution was removed and the plugs were allowed to incubate in the specific repair enzyme buffer for one hour (either Endonuclease III or Fpg). During this incubation period an enzyme working solution (1unit/µl of enzyme, 18 µl of enzyme buffer, 3 µl of 100X DDT) was made. The plugs were then placed into the working enzyme solution for an hour at 4°C and then 65 minutes at 37˚C. The plugs were again given three separate washes in the stop solution of 70 mM Hepes-KOH, 100 mM KCl, and 100 mM EDTA, at a pH of 7.6 for one hour, and then followed by an hour wash in TE buffer, and a wash in 0.5X TBE (45 mM Tris base, 45 mM boric acid, and 1 mM Na2-EDTA, pH 7.8) (Peddi 2008). Using a scalpel the plugs were cut so that they could be placed into the wells of the gel that were used in the pulse field device. The pulse field chamber was filled with 0.25X TBE running buffer. The PFGE process used two separate cycles. The first cycle was set at 3 volts and lasted for 48 hours. The second cycle which immediately followed the first was set at 6 volts and lasted for five hours. Following this the gel was removed and then stained by soaking it in 1 µg/ml ethidium bromide (20 µl/200 ml) for 15 minutes with slight agitation. The gel was then washed with distilled water overnight. Using a FlourChem 8800 imaging system (Alpha Innotech, San Leandro, CA) a photograph of the PFGE gel was taken. The images taken were analyzed using the software Quantiscan (BioSoft, Cambridge, UK), and NALA calculations (Tsao 2007, Peddi 2008, Sutherland 2000). This software and NALA calculations as previously described allowed for numeric comparisons of DNA repair between the differing conditions.

Statistical Significance

Paired Students T-tests was used to evaluate differences between averages of different groups ($P<0.05$).

RESULTS

Measurement of single DNA lesions

Alkaline comet assay was used to evaluate the role of DNA-PKcs in single DNA lesion repair.

Repair of these lesions was studied following oxidative damage (H_2O_2 exposure) using IC86621

treated and non-treated MO59K and MCF7 cells, and MO59J cells as well (Figures 8-13).

Alkaline comet assay methods in conjunction with CometScore^{TM} software (Tritek Corp., VA)

was use to examine tail moments (TM) in cells being studied (See Figure 23 for photographic

examples). Figures 8-10 show the study of repair in IC86621 treated and non-treated MO59K

and MO59J cells following H_2O_2 exposure. Figures 11-13 show the study of repair in IC86621

treated and non-treated MCF7 cells following H_2O_2 exposure. Figure 11 shows the processing of

SSBs was not affected in IC86621 treated MCF7 cells compared to non-treated MCF7cells.

However, as can be seen in figure 8, compared to non-treated MO59K cells, the IC86621 treated

MO59K cells showed a decrease in SSB repair, as did MO59J cells (*; p<0.05). Following H_2O_2

exposure, use of EndoIII and Fpg repair enzyme treatments resulted in greater TM at initial times

(Figure 9-10 and 12-13). Inhibitor treated MO59K and MCF7 cells, and MO59J cells showed

deficient processing of Fpg and EndoIII sites. In comparing EndoIII and Fpg sites it was seen

EndoIII damaged sites were more common at the initial time for all cell lines. This suggested

improperly functioning BER, and/or that H_2O_2 exposure mainly causes oxidized pyrimidines.

Immunoblotting of XRCC1 expression

Immunoblots seen in figures 14-16 show the measured expression of the BER protein XRCC1

following H_2O_2 oxidative damage in IC86621 treated and non-treated MCF7 and MO59K cells,

and in MO59J cells as well. Beta-Actin was used as a loading control. XRCC1 expression levels were decreased in cells whose DNA-PKcs activity was inhibited using IC86621 (see Figures 14 and 16). Since XRCC1is a BER protein (Kashishian 2003) this corresponds with the poor repair of single lesions seen in the DNA-PKcs inhibited cells. MO59J cells which do not express DNA-PKcs had reduced XRCC1 expression as well. However, the reduction in XRCC1 expression was not as prominent in the MO59J cells as it was in the IC86621-treated MO59K cells. Basal levels of XRCC1 expression were increased in DNA-PKcs inhibited cells (Figure 14, lanes 3 and 4). However, as seen in lanes 2 and 4 of Figure 15, the basal level of XRCC1 in the MO59J cells was lower than the basal XRCC1 level seen in MO59K cells, conferring with studies by Toulany et al. (Toulany 2008)

Measurement of DSB and OCDL Repair

The NHEJ pathway functions to repair DSBs, and DNA-PK is an important part in that pathway (Burma 2006, Hudson 2005, Peddi 2008, Smith & Jackson 1999). PFGE in combination with base repair enzymes and NALA calculations were used to study whether DSB and/or OCDL repair following 5Gy irradiation was impacted by DNA-PKcs deficiency. To do this MCF7 and MO59K cells were studied with and without treatments of kinase inhibitors specific for DNA-PKcs. MO59K cells were treated with the inhibitor IC86621, and MCF7 cells were treated with the inhibitor NU7026. MO59J cells were used in the study as a control alongside MO59K cells. MO59J cells do not express DNA-PKcs, making them less efficient in DSB repair. However, except for this non-expression of DNA-PKcs, MO59J cells are otherwise isogenic with MO59K cells (Lees-Miller 1995, and Dibiase 2000).

Over incremental repair times (0, 1, 6, 12, 24, 48 hrs) NU7026-treated MCF7 and IC86621-treated MO59K cells showed significant persistence of DSB compared to their controls (see Figures 17 and 20). The number of DSBs was consistently significantly greater for repair times between 6 to 24 hours post irradiation for inhibitor treated MO59K and MCF7 cells compared to their non-inhibitor treated controls. Even though not statistically significant, the IC86621-treated MO59K cells continually showed a greater DSB accumulation than the MO59J cells. In all experimental cells, DSBs still present 24 hours following irradiation suggests DNA-PKcs deficiencies are resulting in the DNA not being fully rejoined.

Quantification of clustered lesions studied using PFGE can be seen in Figures 18-19 and 21-22. Significant differences in repair between 6-48 hours ($p < 0.05$) were detected between non-inhibitor treated controls and DNA-PKcs deficient cells (IC86621-treated MO59K, NU7026-treated MCF7, and MO59J). As was the case with DSB damage, the IC86621-treated MO59K cells had a greater accumulation of clustered damage than the MO59J cells, but not a statistically significant difference (Figures 18-19). In all inhibitor treated cells, OCDLs did not return to background levels before the final time point (Figures 18-19 and 21-22). A similar trend is seen in figures 18 and 19 for MO59J cells.

DISCUSION

The goal of this study was to examine the involvement of DNA-PK in repair of non-DSB

clustered oxidative DNA damage. Results of this study and others have shown that DNA-PKcs

deficiencies are in fact associated with poor DSB and non-DSB lesion repair. NHEJ and BER

have been shown to function in the repair of non-DSB OCDLs (Hashimoto 2001, Malyarchuk

2008, and Pedi 2008). DNA-PKcs chemical inhibition with highly specific drugs shown to target

exclusively the DNA-PKcs kinase activity was used on DNA-PKcs proficient cells (Baily 2003

and Kashishian 2003, and Wilmore 2004). Repair was measured and compared between

differing conditions and cells following oxidative stress. Oxidative damage was induced using

low level irradiation for PFGE studies, and H_2O_2 exposure in alkaline comet assay studies.

Western blotting was also performed to evaluate the effect DNA-PKcs expression has on the

expression of the BER repair protein XRCC1. The malignant MO59K and MCF7 cells had

normal DNA-PKcs expression. Alongside the studies for these cells, MO59J cells deficient in

DNA-PKcs were used, and served as a control and a comparison for the drug treated cells.

Single strand break analysis as seen from figures 8 and 11, showed decreased repair in both drug

treated MCF7 and MO59K cells following H_2O_2 exposure. MO59J cells also showed decreased

repair similar to that observed in the drug treated MO59K cells. The lack of SSB repair observed

in MO59J and drug treated MO59K cells compared with the effective SSB processing seen in

normal MO59K cells indicate the use of DNA-PK functioning in the BER pathway, and the

inhibiting effects of IC86621. Figures 9-10 and 12-13 also showed decreased EndoIII and FPG

enzyme site repair in cells with inhibited or deficient DNA-PKcs. All figures showed a large and

significant increase in tail moment with the addition of H_2O_2 indicating the effectiveness of H_2O_2

in creating single strand and oxidized base damage. Repair was observed at 0, 3, and 12 hours

post induced oxidative damage. A greater tail moment is seen for repair enzyme treated cells for

figures 9-10 and 12-13, indicating the presence of endogenous oxidized base damage. Figure 11

also shows very low SSB basal damage for MCF7 cells compared to the MO59K and MO59J

cells indicating less endogenous SSBs in MCF7 cells. The fact that all cell lines showed a

greater propensity for endogenous oxidized damage compared to SSB indicated that oxidized

bases may be the more common form of endogenous damage. As can be seen by comparing fig

11 with figures 12-13 this disparity between endogenous SSBs and oxidized base damage was

much more evident in MFC7 cells. In comparing oxidized base repair with the processing of

SSBs using the MCF7 cells the DNA-PKcs inhibited cells showed limited processing ability of

damaged repair enzyme sites. The disproportionately poor enzyme site repair compared to SSB

seen in the MCF7 cells (figures 11-13), indicates that although DNA-PKcs plays some role in

SSB repair it may be of significant importance in the repair of oxidized bases and abasic sites.

The decrease seen in SSB processing efficiency in DNA-PKcs inhibited or absent cells

implicates it as a possible activator of known BER proteins. XRCC1 is a BER protein

previously believed to associate with DNA-PK (Thompson 1990, and Mourgues 2007). To

study DNA-PK's role in BER proteins, XRCC1 was chosen. Whole cell lysates of MO59J cells,

and MO59K and MCF7 cells both treated and non-treated with IC86621 were made following

oxidative damage. As seen in figures 14-16 although XRCC1 expression is present in all

samples. Figures 14 and 16 show that the expression of XRCC1 is decreased in IC86621 treated

samples. Figure 15 shows this is also the case in cells absent for DNA-PKcs. Studies have

shown that XRCC1 expression levels following damage may be related to the base expression of

XRCC1 in undamaged cells, and that cells with low basal expression have larger increases in

XRCC1 expression following oxidative damage (Toulany 2008). It is believed that DNA-PK

does not activate XRCC1 production, but either stabilizes or activates and regulates present

XRCC1 in response to oxidative damage (Toulany 2008). It cannot be ruled out that DNA-PKcs

has some effect on synthesis of new XRCC1. However, studies have shown that the quick

induction of XRCC1 following damage indicates a stabilizing or activating role of DNA-PKcs

(Toulany 2008).   XRCC1 has shown to be quickly degraded by the ubiquitin-protease pathway

and that the protein JWA stabilizes XRCC1 by blocking ubiquilyation sites (Wang 2009). It is

possible that DNA-PKcs could serve a similar role or even have some function with JWA or

proteins like it to stabilize XRCC1. None the less, studies have implicated XRCC1 as vital in

base lesion repair (Mourgues 2007). The decreased XRCC1 expression in the blot samples

deficient in DNA-PKcs coupled with the decreased processing of repair enzyme sites seen in

figures 9-10 and 12-13 help to give credence to XRCC1's role in base lesion repair. This

additionally provides a possible expiation for the poor repair seen in the enzyme treated samples.

Double strand break analysis was performed on post 5Gy γ-irradiated MO59K, MO59J, and

MCF7 cells with identical drug treatment conditions used in the SSB studies previously

described. Similar differences were seen in DSB repair analysis (figures 17-22). Again there appeared to be decreased repair in DNA-PKcs inhibited/absent. DSBs are more complex to repair than single lesions (Jackson 2002). Unlike the SSB results (Figures 8-13) this difference in repair between the samples is not significant until time points of six hours or more. Notice that at initial time points all samples of each condition show similar amounts of damage, and that by the final time point all cells expressing DNA-PKcs have nearly returned to basal levels of damage. Repair ability appears to be decreased for oxidized base lesions particularly for Fpg sites. As seen in figure 19, not only did the DNA-PKcs inhibited/absent cells have decreased repair, their number of DSBs resulting from oxidized purines increased in the final hours. Considerably less efficient repair in the drug treated MO59K and MO59J cells was seen compared to non-treated MO59K cells. To ensure the decreased repair was due to DNA-PKcs inhibition and not solely a novel attribute of IC86621, another DNA-PKcs inhibitor (NU7426) was used with the MCF7 cells. As seen in figures 20-22, again a decreased ability to processes DSB's is seen in the drug treated samples. Again the initial time point shows that the cells had a similar damage response to the irradiation treatment and that by the final time point the untreated samples had nearly returned to their basal level, whereas the drug treated samples still possessed much unprocessed damage.

The decrease in DSB and base lesion repair efficiency adds to the evidence suggesting that DNA-PK has a role in the NHEJ and HR (Hashimoto 2001, Malyarchuk 2008, Allen 2003). It also indicates poor OCDL repair in response to DNA-PK deficiencies. Interestingly, the

decreased repair efficiency seen in drug treated MO59K cells was greater than the decrease seen in the MO59J cells. These differences suggest that the inhibitor may affect proper functioning of other repair pathways that are allowed to operate in MO59J cells. Drugs such as IC86621 do not inhibit the production of DNA-PKcs, but inhibit its kinase ability. Therefore DNA-PKcs is still able to be recruited to damaged sites, but unable to dissociate (Meek 2007, Meek 2008, Shrivastav 2008). As time progresses damage continues to be repaired. This repair is slowed in DNA-PKcs deficient cells and even more delayed in DNA-PKcs inhibited cells. This data, coupled with current knowledge of the role of DNA-PK in repair, indicates different models may exist for complex DNA damage repair (figure 24).

This study helps to better understand the role of DNA-PK in the repair of clustered DNA lesions. Results from SSB, DSB and abasic site repair analysis indicate that cells with inhibited or absent DNA-PKcs exhibit compromised lesion repair. These results indicate the possible employment of DNA-PK in the functioning of different repair pathways. Proteins kinases help regulate the cycle and proper maintenance of cells including their genomic repair (Fabbro 2002 and Kiahishian 2003). With various protein kinases having been linked to genes important in cancer prevention, the research of protein kinase inhibition in cancer treatment is a growing field of study (Fabbro 2002). Many cancer treatments induce DNA damage to levels lethal to cells. Therefore, for those targeted cells less efficient repair would be preferred. This and other studies have shown that DNA-PKcs inhibition results in poor DNA repair, and increases cell sensitivity to radiotherapy and chemotherapeutics such as Bleomycin. Thus, suggesting possible benefits of

DNA-PKcs inhibition in cancer treatments (Kashisian 2003). This study shows that using chemical inhibition of DNA-PKcs in malignant tumor cells results in a decrease in the cells ability to repair damage. These results indicate the importance of DNA-PK in the repair of DNA, and therein its role in maintaining genomic integrity.

Figure 8. The effect of DNA-PKcs inhibition in the repair of SSBs. SSB repair in IC86621 and

H_2O_2 treated MO59K cells and regular MO59J/K cells and control following 15 min exposure to

100 µM H_2O_2. The control with no H_2O_2 and no IC6621 is included. SSB detection at 0, 3 and

12 hrs following damage using alkaline single cell gel electrophoresis (comet assay). Values are

averages from 3 independent experiments. Statistically significant differences between IC86621

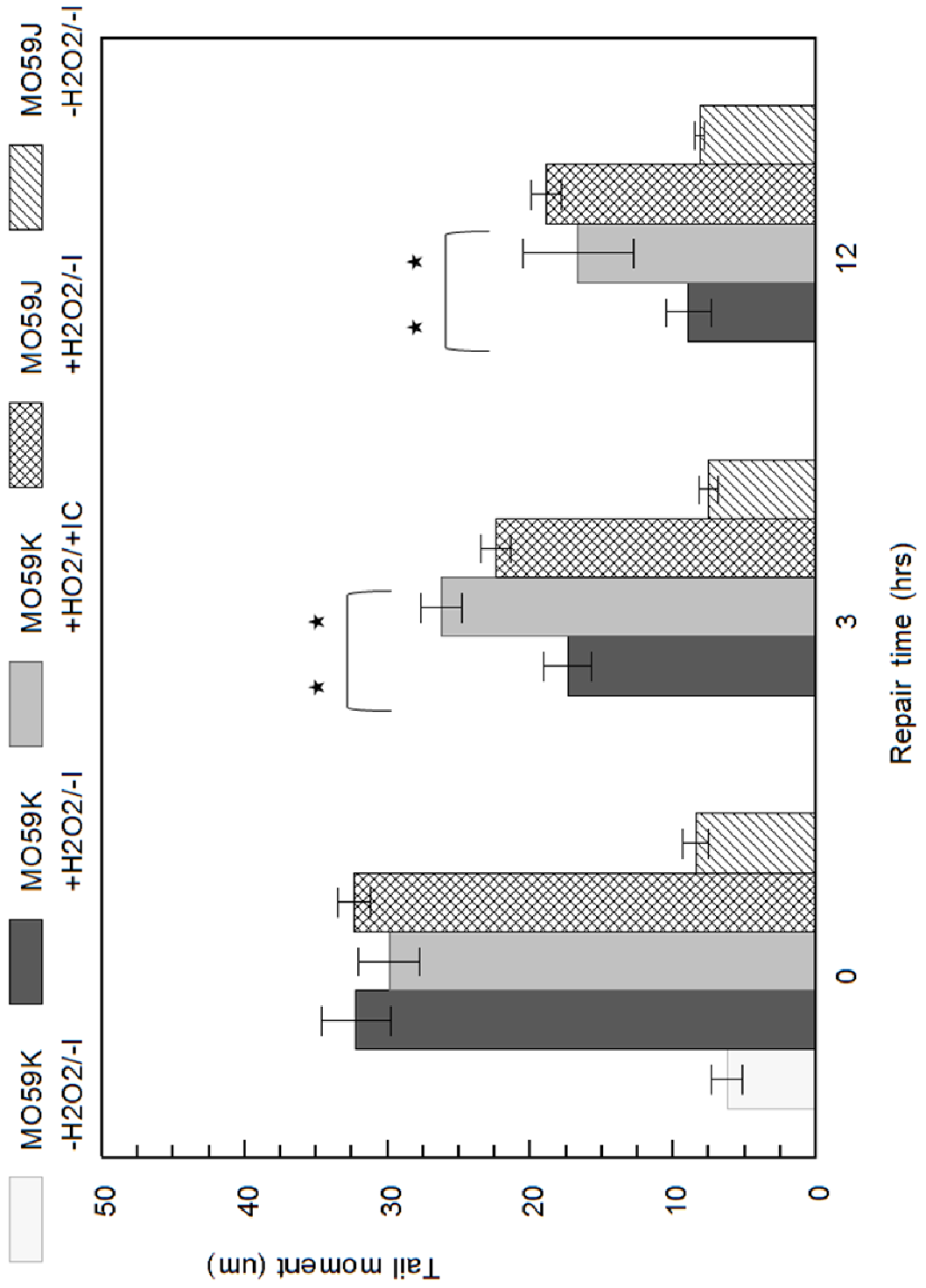treated MCF7 cells and controls at $p < 0.05$ are depicted by (*).

# Single Strand Break Alkaline Comet Analysis

Legend:
- MO59K -H2O2/-IC
- MO59K +H2O2/-IC
- MO59K +H2O2/+IC
- MO59J +H2O2/-IC
- MO59J +H2O2/+IC
- MO59J -H2O2/-IC

Y-axis: Tail moment (um)

X-axis: Repair time (hrs)
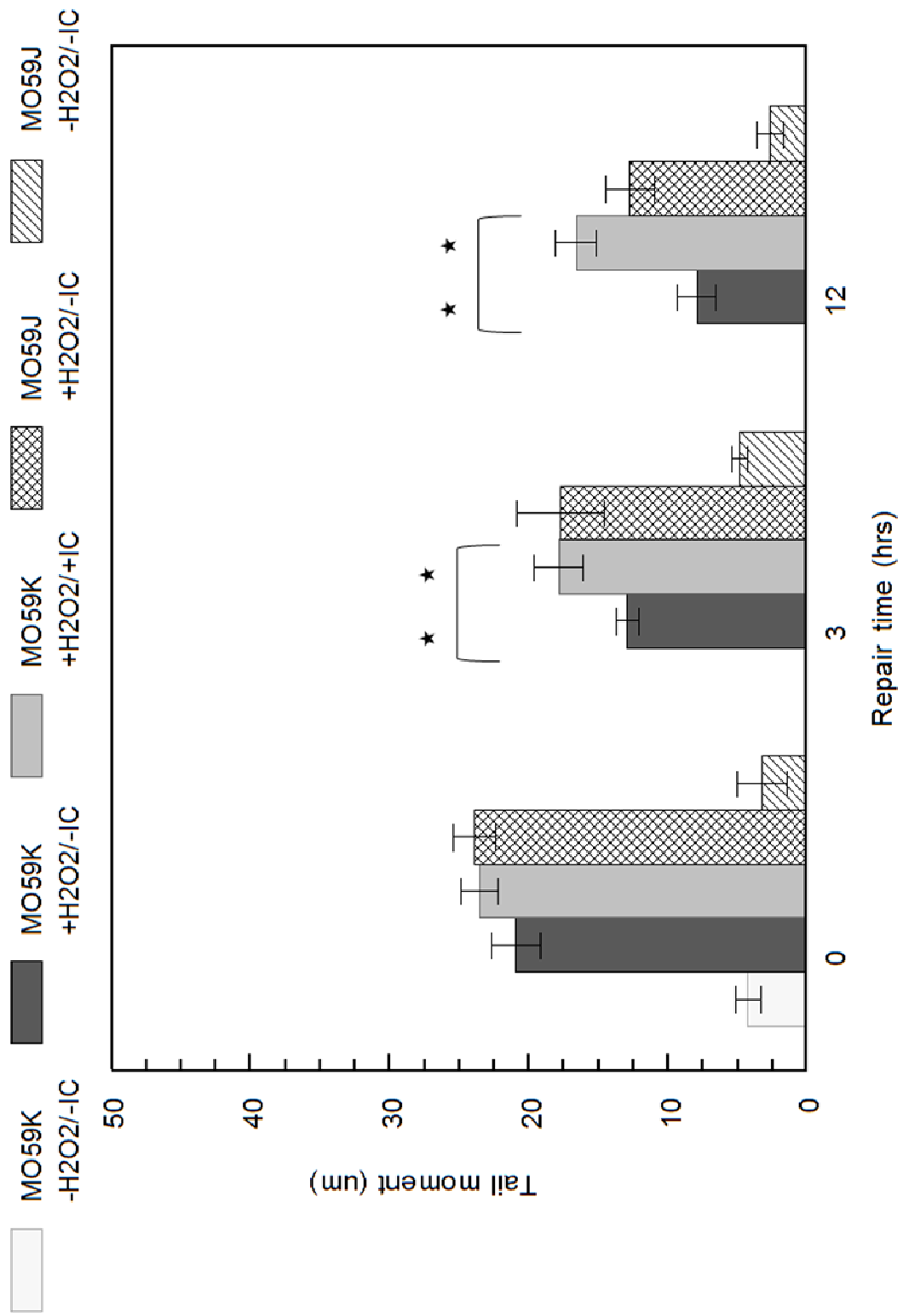
Figure 9. The effect of DNA-PKcs inhibition in the repair of oxidized bases. Repair of oxidized

pyrimidines in IC86621 and H_2O_2 treated MO59K cells and regular MO59J/K cells and control

following 15 min exposure to 100 µM H_2O_2. The control with no H_2O_2 and no IC86621 is

included. EndoIII site detection at 0, 3 and 12 hrs following damage using alkaline single cell

gel electrophoresis (comet assay). Values are averages from 3 independent experiments.

Statistically significant differences between IC86621 treated MCF7 cells and controls at $p<0.05$

are depicted by (*).

EndoIII Lesion Alkaline Comet Analysis
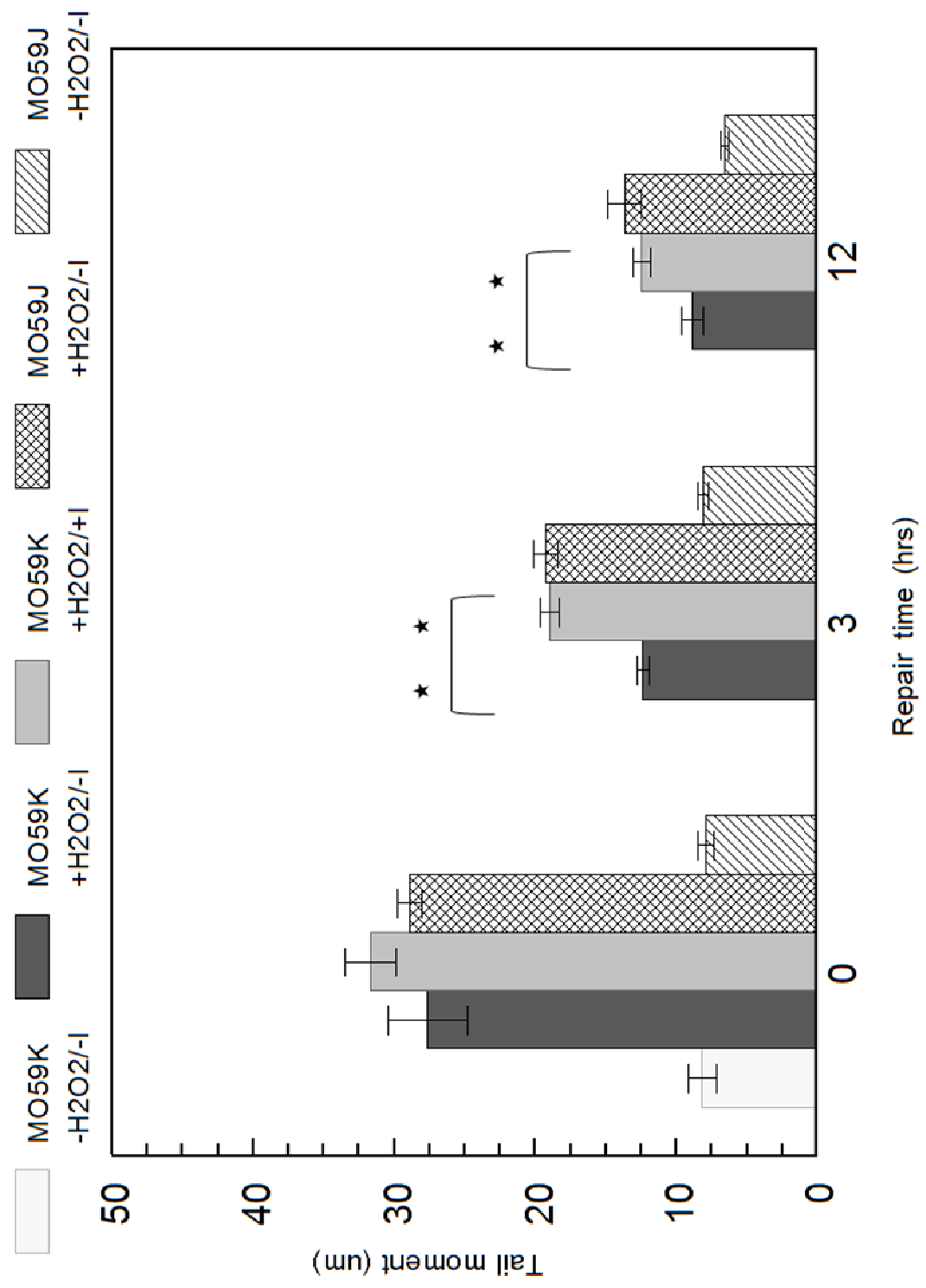
Figure 10. The effect of DNA-PKcs inhibition in the repair of oxidized bases. Repair of oxidized purines in IC86621 and H_2O_2 treated MO59K cells and regular MO59J/K cells and control following 15 min exposure to 100 µM H_2O_2. The control with no H_2O_2 and no IC86621 is included. Fpg site detection at 0, 3 and 12 hrs following damage using alkaline single cell gel electrophoresis (comet assay). Values are averages from 3 independent experiments. Statistically significant differences between IC86621 treated MCF7 cells and controls at $p<0.05$ are depicted by (*).
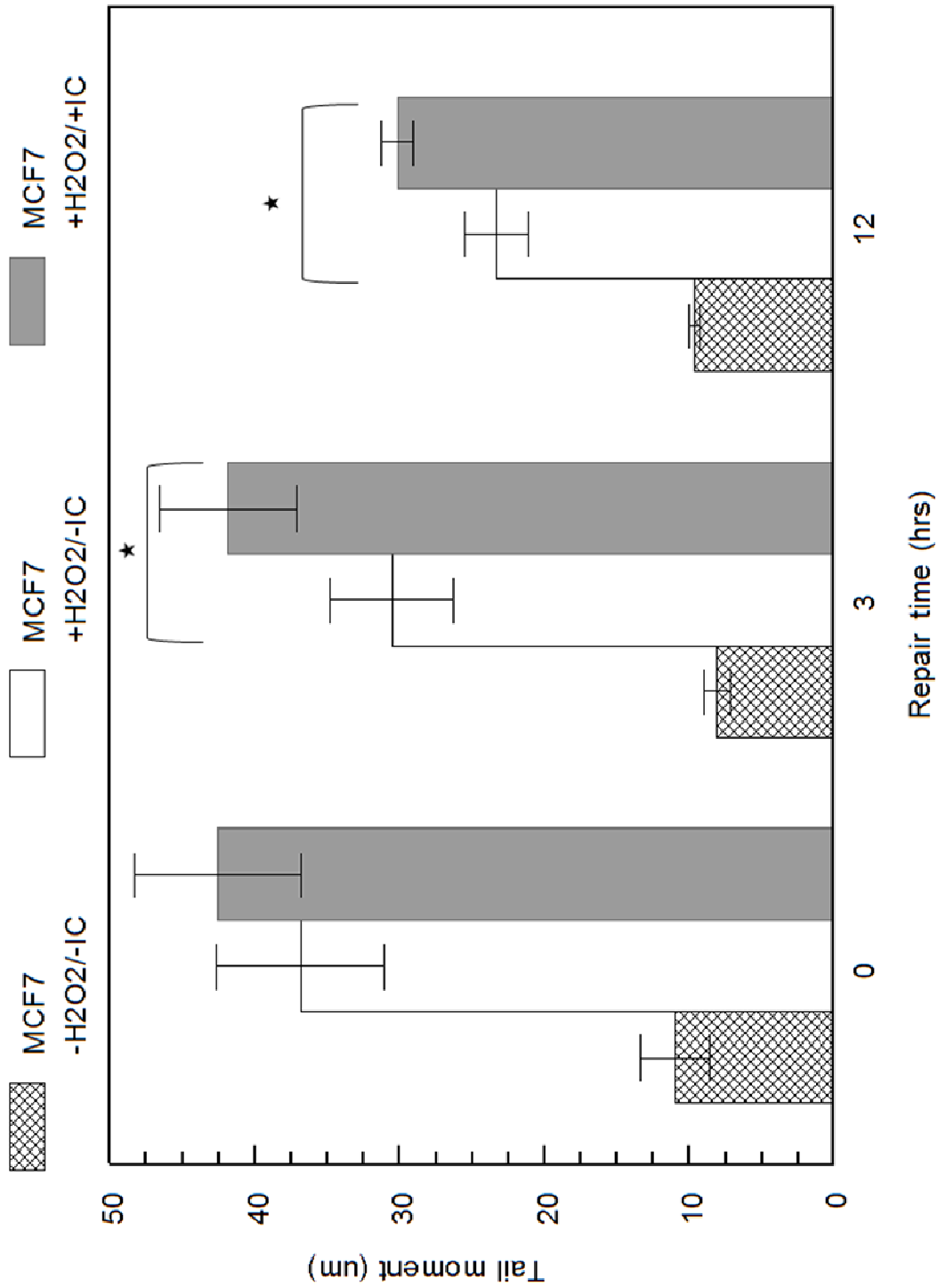
Fpg Lesion Alkaline Comet Analysis

Figure 11. The effect of DNA-PKcs inhibition in the repair of SSBs. Single lesion repair in IC86621 and H_2O_2 treated MCF7 cells and controls following 15 min exposure to 100 μM H_2O_2. The control with no H_2O_2 and no IC6621 is included. SSB break detection done at 0, 3 and 12 hrs following damage using alkaline single cell gel electrophoresis (comet assay). Values are averages from 2 independent experiments. Statistically significant differences between IC86621 treated MCF7 cells and controls at $p < 0.05$ are depicted by (*).

Single Strand Break Alkaline Comet Analysis
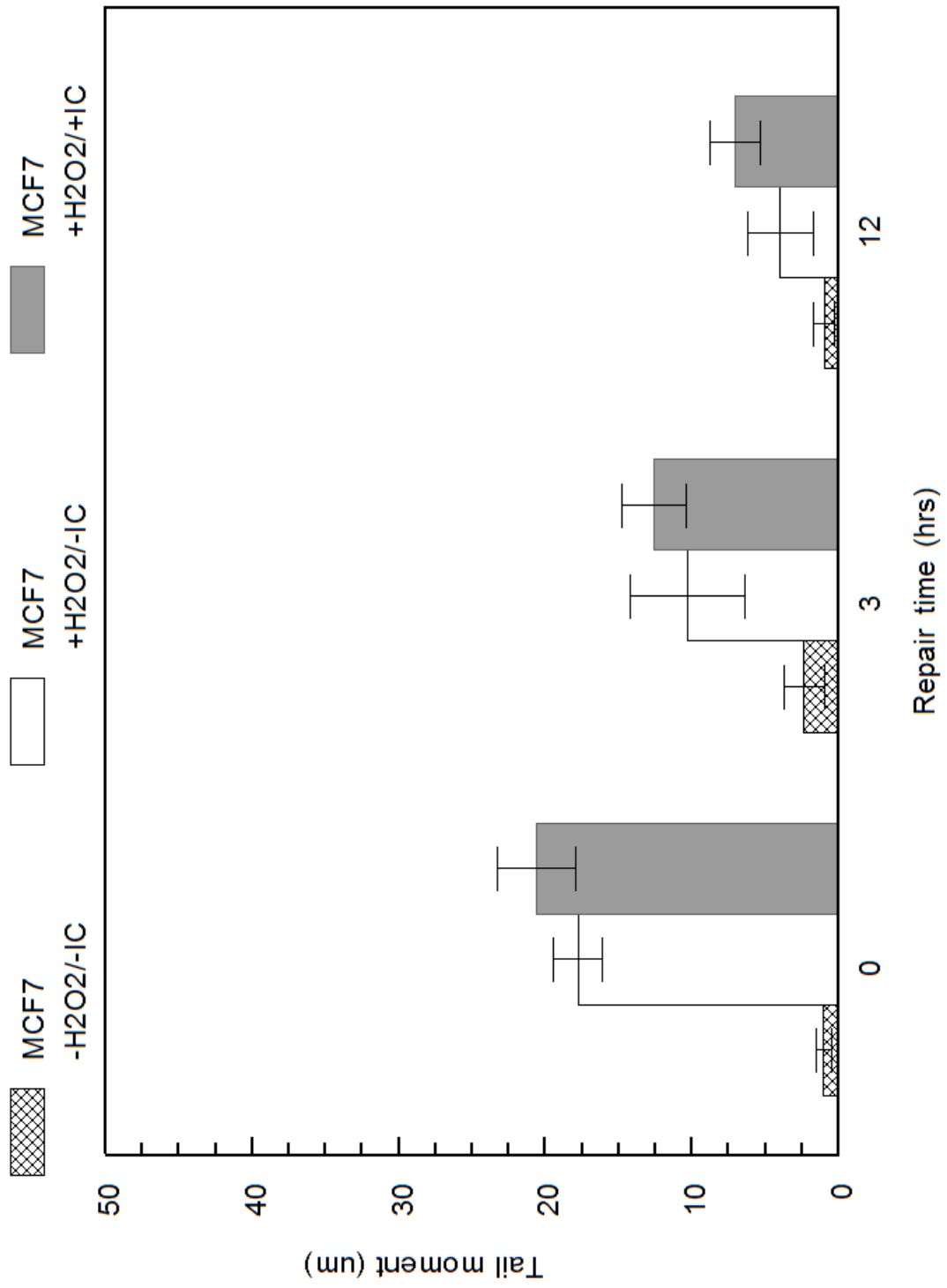
Figure 12. The effect of DNA-PKcs inhibition in the repair of single oxidative DNA lesions. Oxidized pyrimidine repair in IC86621 and H_2O_2 treated MCF7 cells and controls following 15 min exposure to 100 µM H_2O_2. The control with no H_2O_2 and no IC6621 is included. EndoIII site detection at 0, 3 and 12 hrs following damage using alkaline single cell gel electrophoresis (comet assay). Values are averages from 2 independent experiments. Statistically significant differences between IC86621 treated MCF7 cells and controls at $p<0.05$ are depicted by (*).

Endoll Lesion Alkaline Comet Analysis

45

Figure 13. The effect of DNA-PKcs inhibition in the repair of single oxidative DNA lesions. Oxidized purine repair in IC86621 and H_2O_2 treated MCF7 cells and controls following 15 min exposure to 100 µM H_2O_2. The control with no H_2O_2 and no IC6621 is included. Fpg site detection at 0, 3 and 12 hrs following damage using alkaline single cell gel electrophoresis (Comet Assay). Values are averages from 2 independent experiments. Statistically significant differences between IC86621 treated MCF7 cells and controls at $p<0.05$ are depicted by (*).

Fpg Lesion Alkaline Comet Analysis

47
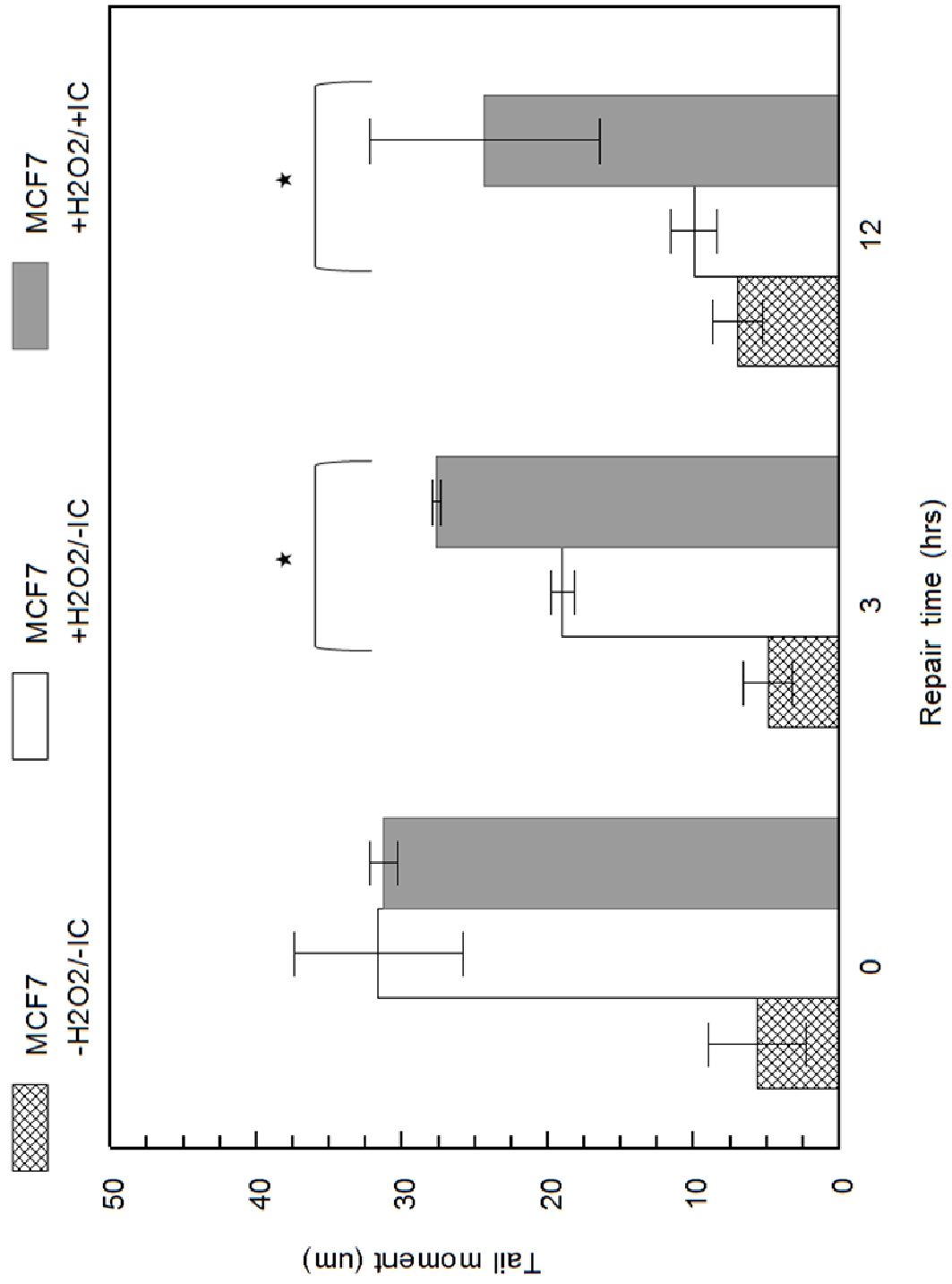
Figure 14. Western blot detection of XRCC1 in IC86621 treated MCF-7 cells 30 min following

100 µM H_2O_2 exposure. Each lane contained 40 µg of protein. Lane 4 (MCF7 with DMSO)

served as control. β-actin was used as a loading control. Values were normalized to the control
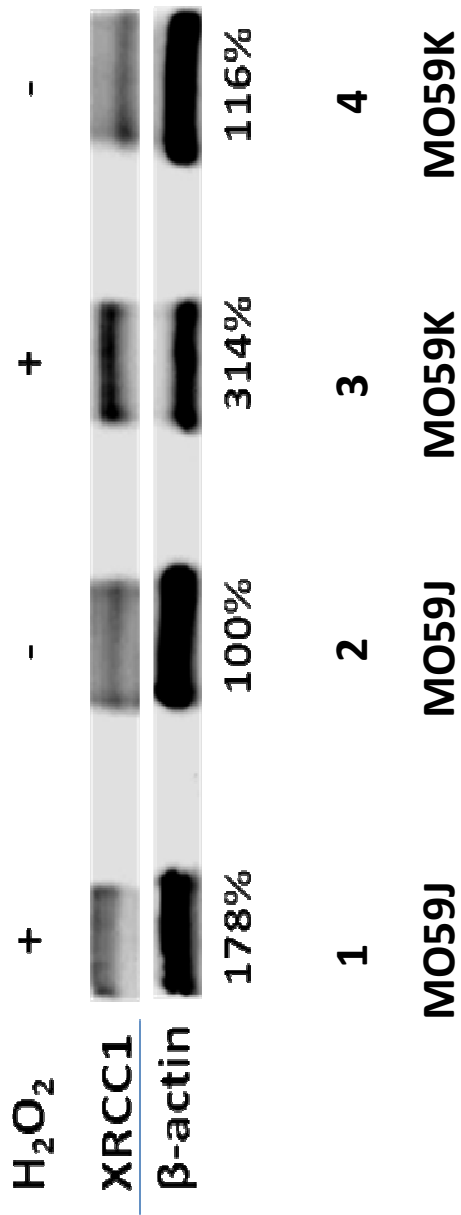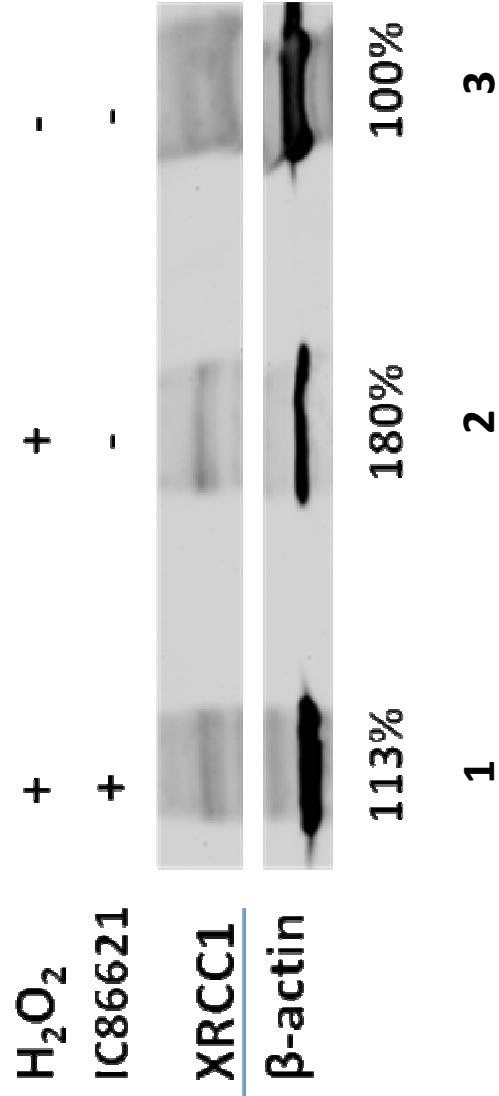
and shown as the ratio of XRCC1/actin.

MCF-7 Cells

	1	2	3	4
H_2O_2	+	+	-	-
IC86621	-	+	+	-
XRCC1	576%	204%	132%	100%

49
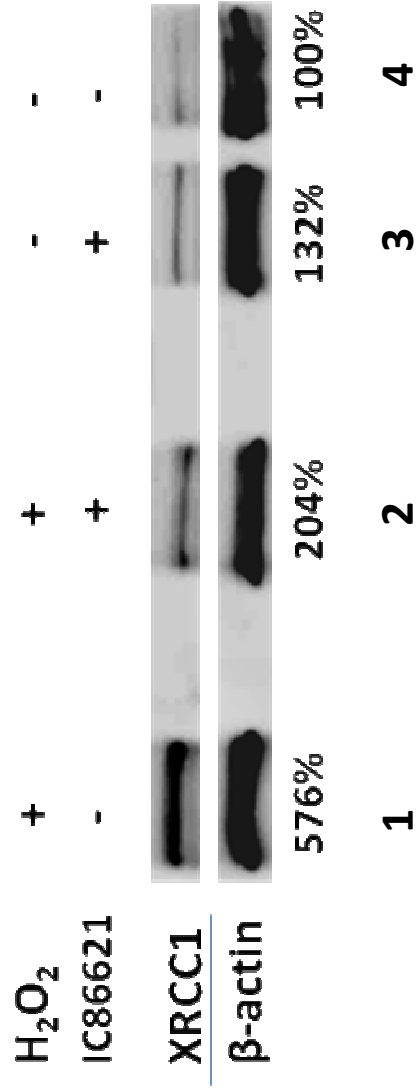
Figure 15. Western blot detection of XRCC1 in IC86621 treated MO59J/K cells 30 min

following 100 µM H_2O_2 exposure. Each lane contained 40 µg of protein. Lane 2 (MO59J with no

H_2O_2) served as control. β-actin was used as a loading control. Values were normalized to the

control and shown as the ratio of XRCC1/β-actin.

MO59K and MO59J Cells

H$_2$O$_2$	+	-	+	-
XRCC1				
β-actin	178%	100%	314%	116%
	1	2	3	4
	MO59J	MO59J	MO59K	MO59K

Figure 16. Western blot detection of XRCC1 in IC86621 treated MO59K cells 30 min following

100 µM H_2O_2 exposure. Each lane contained 40 µg of protein. Lane 3 (MO59K with DMSO

only) served as control. β-actin was used as a loading control. Values were normalized to the

control and shown as the ratio of XRCC1/β-actin.

MO59K Cells

	1	2	3
H$_2$O$_2$	+	+	-
IC86621	+	-	-
XRCC1			
β-actin	113%	180%	100%

Figure 17. Detection of DSB damage repair using PFGE. Processing of DSBs as a function of

time following irradiation in DNA-PKcs proficient MO59K cells and in deficient MO59J and

IC86621 treated MO59K cells. Averaged values from independent experiments for MO59K and

MO59J cells were taken at 0, 1, 6, 12, 24, and 48 hrs. In some instances SEM error bars are

smaller than their associated symbol. MO59K cells are Square symbols. MO59J cells are

circular symbols. MO59K cells treated with IC86621 are Triangular symbols. Statistically

significant differences between IC86621 treated MCF7 cells and controls at $p<0.05$ are depicted

by (*).
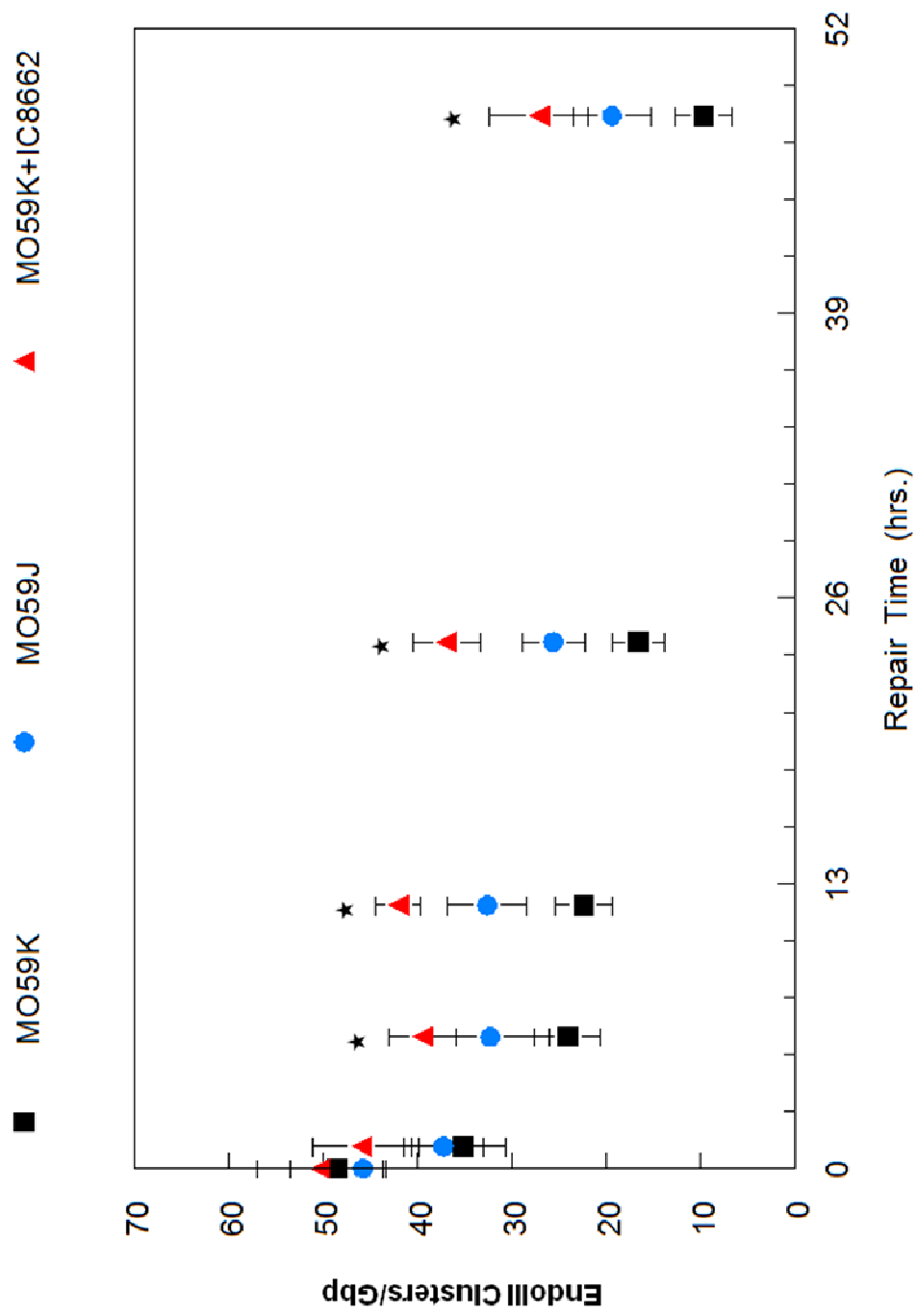
Double Strand Break Analysis
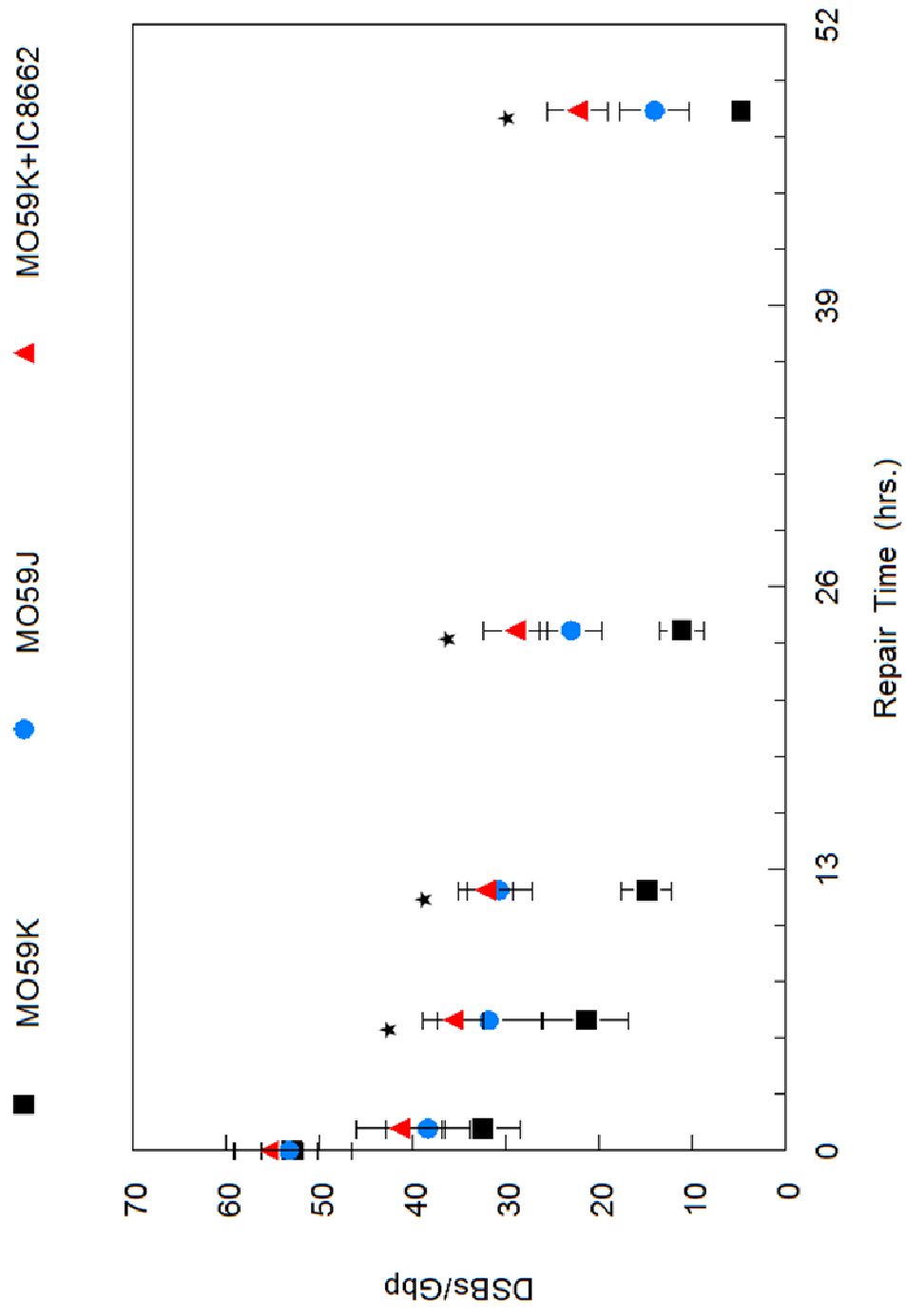
Figure 18. Detection of non-DSB oxidized cluster repair using PFGE. Processing of pyrimidine damage as a function of time following irradiation in DNA-PKcs proficient MO59K cells and in deficient MO59J and IC86621 treated MO59K cells. Averaged values from independent experiments for MO59K and MO59J cells were taken at 0, 1, 6, 12, 24, and 48 hrs. In some instances SEM error bars are smaller than their associated symbol. MO59K cells are Square symbols. MO59J cells are circular symbols. MO59K cells treated with IC86621 are Triangular symbols. Statistically significant differences between IC86621 treated MCF7 cells and controls at $p < 0.05$ are depicted by (*).

EndoIII Cluster Analysis

■ MO59K   ● MO59J   ▲ MO59K+IC8662

EndoIII Clusters/Gbp

Repair Time (hrs.)

Figure 19. Detection of non-DSB oxidized cluster repair using PFGE. Processing of purine damage as a function of time following irradiation in DNA-PKcs proficient MO59K cells and in deficient MO59J and IC86621 treated MO59K cells. Averaged values from independent experiments for MO59K and MO59J cells were taken at 0, 1, 6, 12, 24, and 48 hrs. In some instances SEM error bars are smaller than their associated symbol. MO59K cells are Square symbols. MO59J cells are circular symbols. MO59K cells treated with IC86621 are Triangular symbols. Statistically significant differences between IC86621 treated MCF7 cells and controls at $p < 0.05$ are depicted by (*).
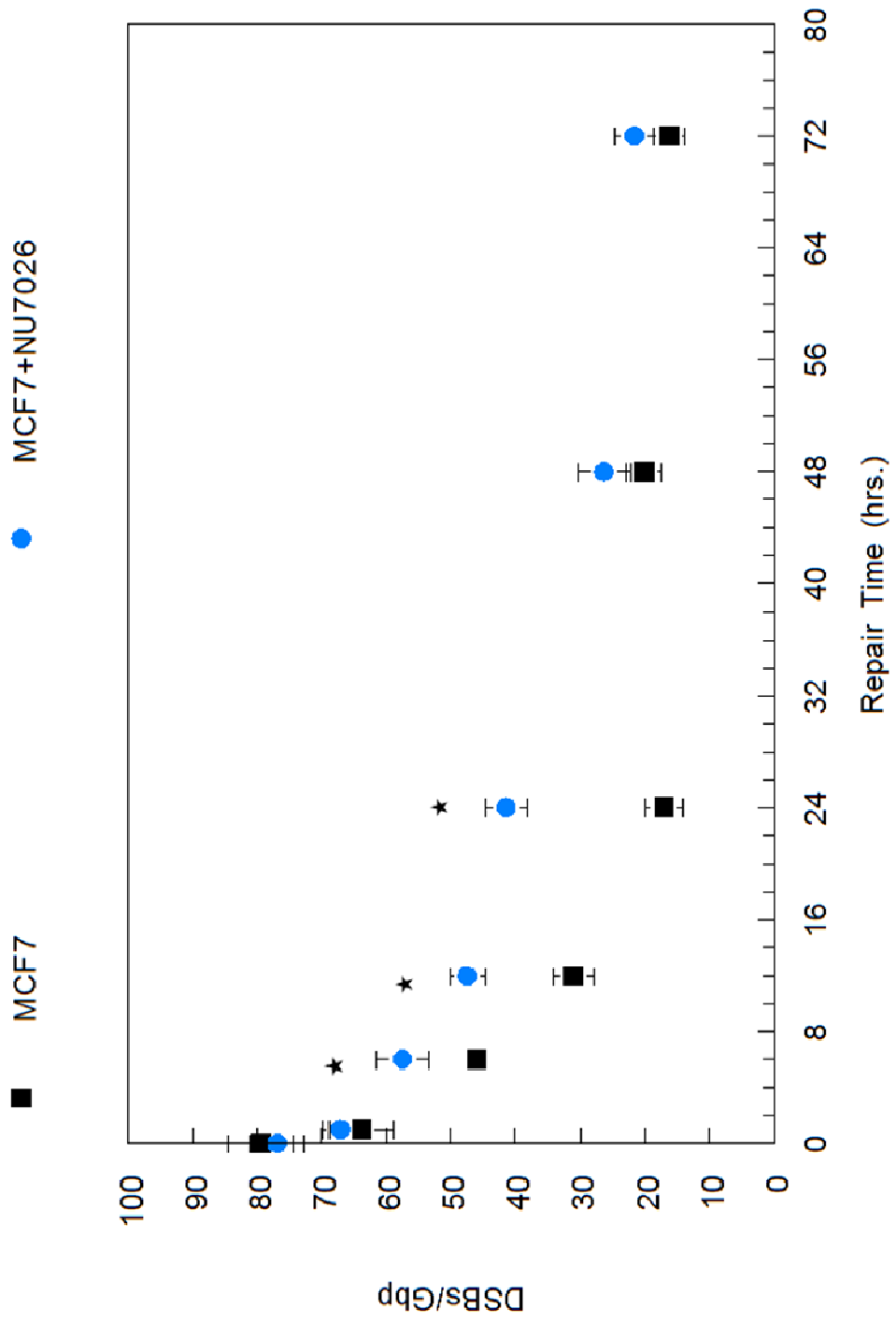
Fpg Cluster Analysis
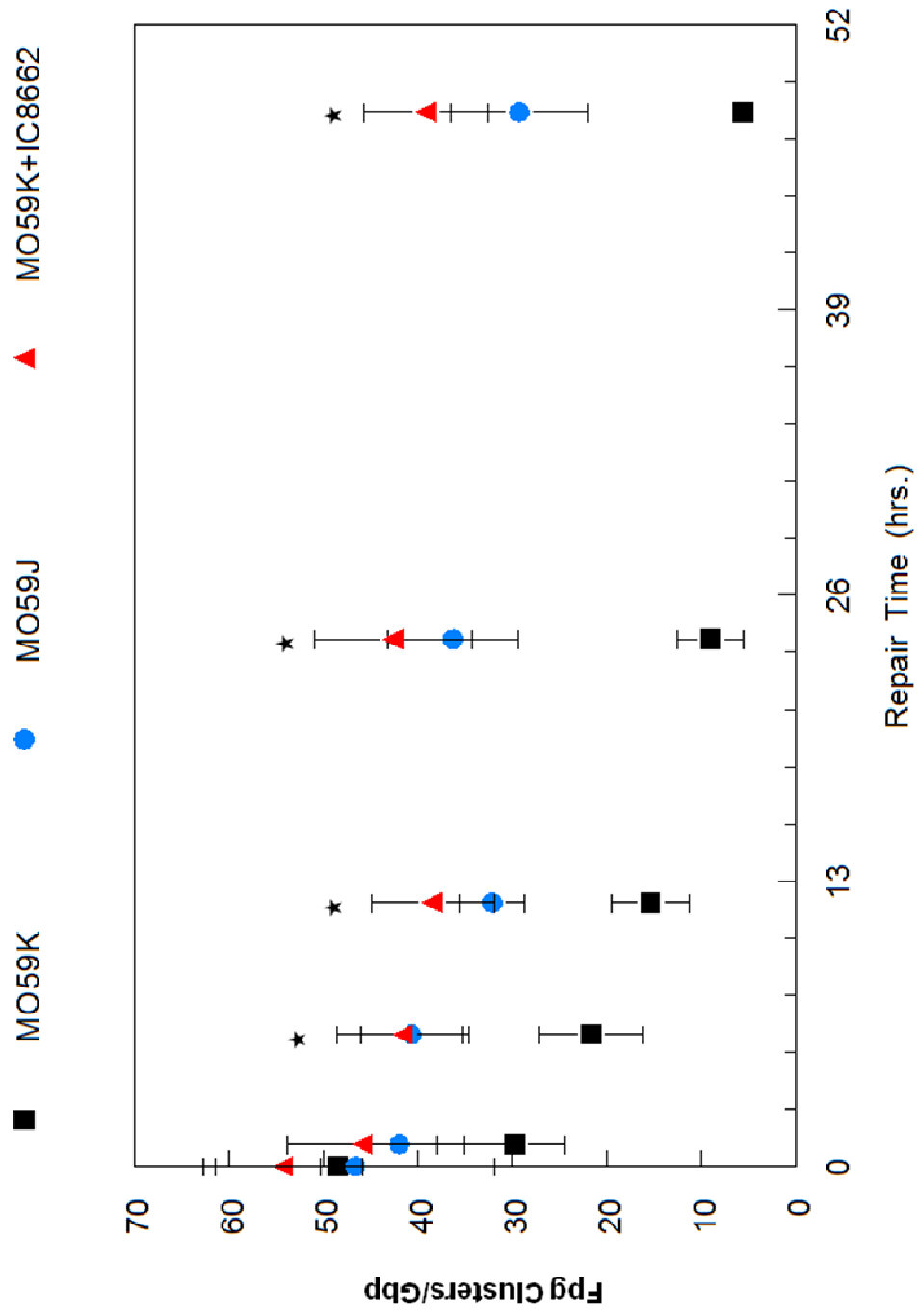
Figure 20. Detection of DSB damage repair using PFGE. Processing of DSBs as a function of time following irradiation in DNA-PKcs proficient MCF7 cells and in inhibited NU7026 treated MCF7 cells. Averaged values from 3 independent experiments for NU7026 treated and non-treated MCF7 cells were taken at 0, 1, 6, 12, 24, and 48 hrs. In some instances SEM error bars are smaller than their associated symbol. Untreated MCF7 cells are square symbols. NU7026 treated MCF7 cells are circular symbols. Statistically significant differences between IC86621 treated MCF7 cells and controls at $p<0.05$ are depicted by (*).
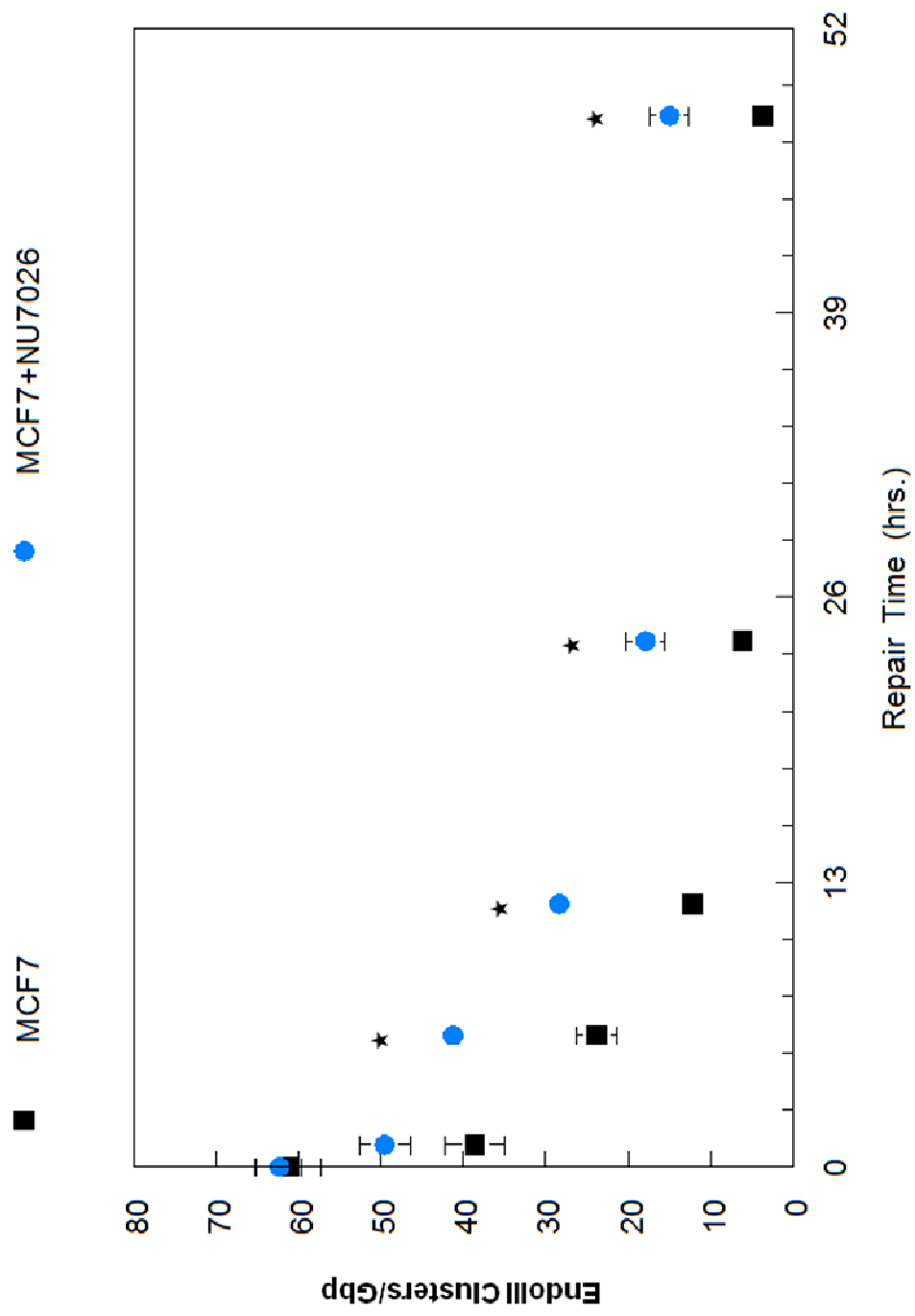
Double Strand Break Analysis

Figure 21. Detection of non-DSB oxidative DNA cluster repair using PFGE. Processing of pyrimidine clusters as a function of time following irradiation in DNA-PKcs proficient MCF7 cells and in inhibited NU7026 treated MCF7 cells. Averaged values from 3 independent experiments for NU7026 treated and non-treated MCF7 cells were taken at 0, 1, 6, 12, 24, and 48 hrs. In some instances SEM error bars are smaller than their associated symbol. Untreated MCF7 cells are square symbols. NU7026 treated MCF7 cells are circular symbols. Statistically significant differences between IC86621 treated MCF7 cells and controls at $p < 0.05$ are depicted by (*).

Endolll Cluster Analysis

Figure 22. Detection of non-DSB oxidative DNA cluster reapir using PFGE. Processing of pyrimidine clusters as a function of time following irradiation in DNA-PKcs proficient MCF7 cells and in inhibited NU7026 treated MCF7 cells. Averaged values from 3 independent experiments for NU7026 treated and non-treated MCF7 cells were taken at 0, 1, 6, 12, 24, and 48 hrs. In some instances SEM error bars are smaller than their associated symbol. Untreated MCF7 cells are square symbols. NU7026 treated MCF7 cells are circular symbols. Statistically significant differences between IC86621 treated MCF7 cells and controls at $p<0.05$ are depicted by (*).
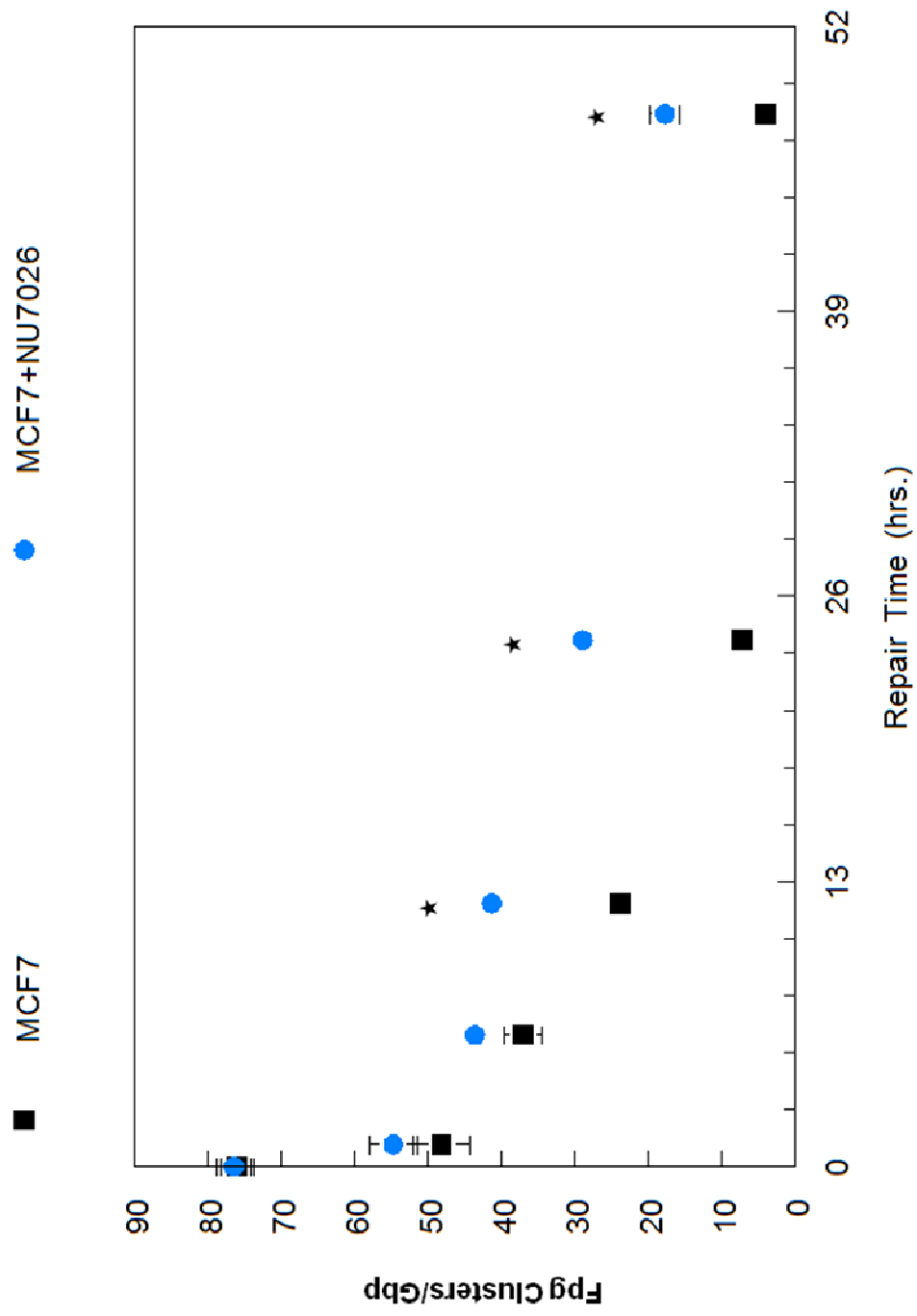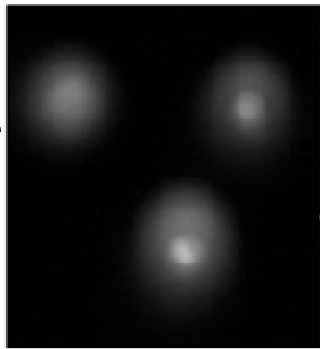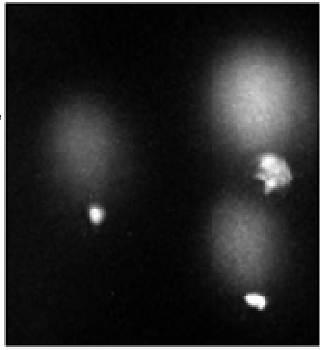
Fpg Cluster Analysis

Figure 23. Photos comparing MO59K cells treated with the DNA-PKcs inhibitor IC86621, and MO59K cells without IC86621. Photos were taken following 100μM H_2O_2 exposure and electrophoresis at $0.7V/cm^2$ taken at 20X magnification. Photos were taken at 0, 3, and 12 hour repair times showing initial damage and the decrease in tail moment as time progresses, and the decreased repair in drug treated cells.
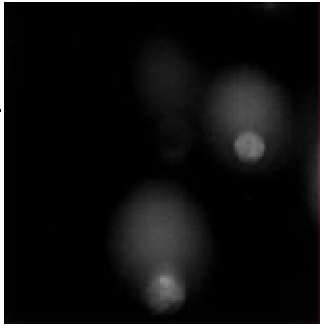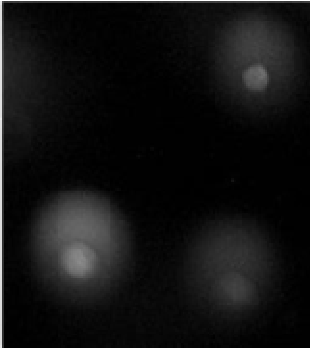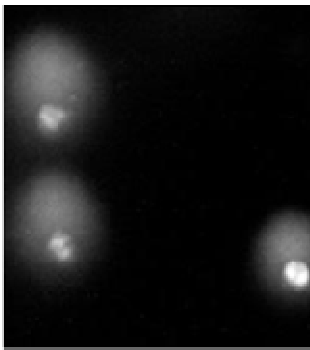
MO59K 0hr with H2O2, with IC86621

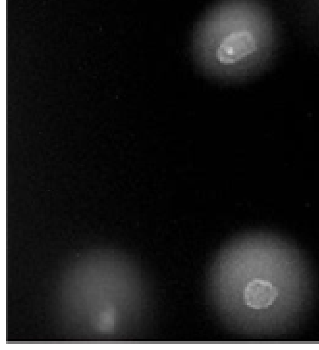MO59K 0hr with H2O2, No IC86621

MO59K 3hr with H2O2, with IC86621

MO59K 12hr with H2O2, with IC86621

MO59K 0hr No H2O2, No IC86621

MO59K 3hr with H2O2, No IC86621
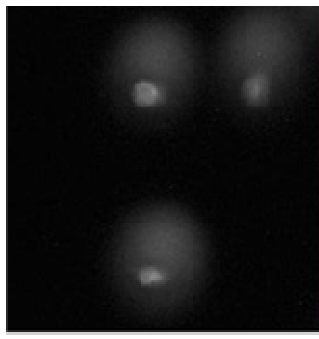
MO59K 12hr with H2O2, No IC86621

67

Figure 24. Representation of differing OCDL processing pathways based on the presence, absence or inhibition of DNA-PKcs activity. Autophosphorylation of DNA-PK allows disassociation from the ends of DNA. This dissociation must happen so DSB repair by NHEJ and HR can ensue, and then other clustered sites can be repaired normally as seen in Path I. Path II shows NHEJ cannot proceed in situations of DNA-PKcs absence so other DSB repair pathways are utilized. Inhibition of DNA-PKcs autophosphorylation due to chemical inhibitors prevents dissociation from the damaged site as seen in Path III. In this situation repair via NHEJ does not occur and DNA-PKcs molecule blocks the site from being properly repaired by other repair pathways. (Courtesy of A.G. Georgakilas)

Processing of oxidatively-induced clustered DNA lesions (OCDLs)

(I)
Normal DNA-PKcs

(II)
Absence of DNA-PKcs

(III)
Inhibition of DNA-PKcs kinase activity (IC86621/NU7026)
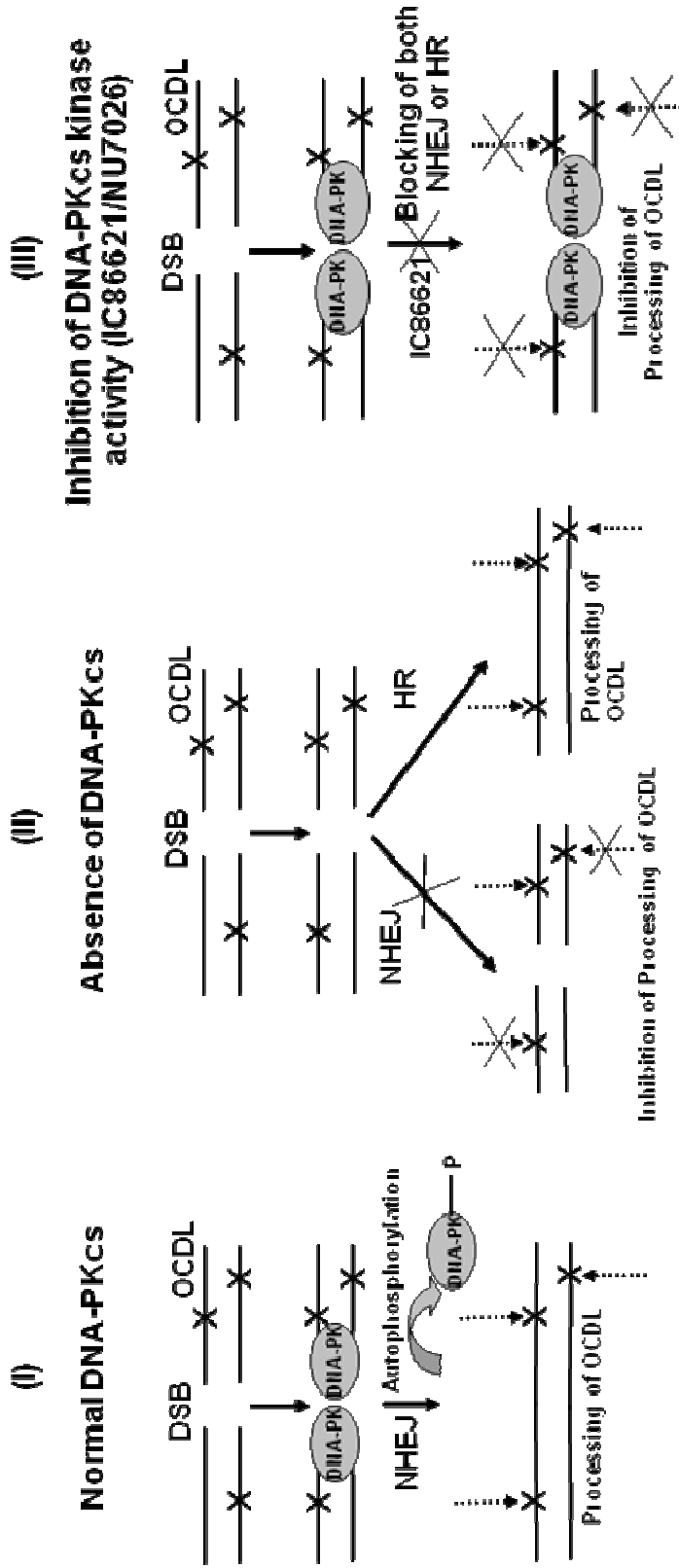

(Courtesy of A.G. Georgakilas)

69

Table 1. A table listing the known oxidative base damage substrates with a repair enzyme known to cleave it. Table shows the oxypyrimidines repaired by EndoIII, and the oxypurines repaired by Fpg (courtesy A. Georgakilas) (Weinfeld 2001, Hada and Georgakilas 2008).

Repair enzymes used as damage probes	Substrates
E.coli Fpg protein or hOGG1 protein (DNA glycosylase) Associated lyase activity	Oxypurines: FapyAdenine, FapyGuanine, C8-oxoGuanine, some abasic sites, C8-oxoAdenine, and other modified purines.
E.coli or human Nth1 protein (Endonuclease III) Associated lyase activity	Oxypyrimidines: Thymine residues damaged by ring saturation, fragmentation, or ring contraction including thymine glycol and uracil residues.

(**Courtesy A. Georgakilas**) (Weinfeld 2001, Hada and Georgakilas 2008)

REFERENCES

Allen, C., Halbrook, J., Nickoloff, J.A. (2003). Interactive competition between homologous recombination and non-homologous end joining. Molecular Cancer Research, 1, 913-920.

Arlander., S.J.H., Greene, B.T., Innes, C.L., Paules, R.S. (2008). DNA protein kinase-dependent G2 checkpoint revealed following knockdown of ataxia-telangiectasia mutated in human mammary epithelial cells. Cancer Research, 68(1), 89-97.

Baily, S.M., Breenneman, M.A., Halbrook, J.M., Nickoloff, J.A., Ulrich, R.L., Goodwin, E.H. (2003). The kinase activity of DNA-PK is required to prevent mammalian telomers. DNA Repair, 3(3), 225-233.

Blöcher, D., Einspenner M., Zajackowski, J. (1989). CHEF electrophoresis, a sensitive technique for the determination of DNA double-strand breaks. International Journal of Radiation Biology, 56(4), 437-448.

Burma, S.; Chen, B. P. C.; Chen, D. J. (2006). Role of Non-homologous End Joining (NHEJ) in maintaining genomic integrity. DNA Repair, 5, 1042-1048.

Cadet, J., Delatour, T., Douki, T., Gasparutto, D., Pouget, J., Ravanat, J., Sauvaigo, S. (1998). Hydroxyl radicals and DNA base damage. Mutation Research, 424, 9-21.

Chan, D.W., and Lees-Miller, S.P. (1996). The DNA-dependent protienkinase is inactivated by autophosphorylation of the catalytic subunit. Journal of Biological Chemistry, 271(15), 8936-8941.

Cooke, M.S., Evans, M.D., Dizdaroglu, M., Lunec, J. (2003). Oxidative DNA Damage: Mutation and Disease. The Federation of American Societies for Experimental Biology Journal, 17, 1195-1214.

Dianov, G.L., O'Neill, P.O., Goodhead, D.T. (2001). Securing genome stability by orchestrating DNA repair: removal of radiation-induced clustered lesions in DNA. BioEssays, 23, 745-749.

DiBiase, S.J., Zeng, C.Z., Chen, R., Hyslop, T., Curran Jr., W.J., Iliakis, G. (2000). DNA-dependent protein kinase stimulates an independently active, nonhomologous, end joining apparatus. Cancer Research, 60, 1245-1253.

Djuric, Z., Evererette, C.K., Luongo, D.A. (1993). Toxicity, single-strand breaks and 5-hydroxymethyl-2'-deoxyuridine formation in human breast epithelial cells treated with hydrogen peroxide. Free Radical Biology and Medicine, 14(5), 541-547.

Douki, T., Ravanat, J.L., Paget, J.P., Testard, I., Cadet, J. (2006). Minor contribution of direct ionization to DNA base damage induced by heavy ions. International Journal of Radiation Biology, 82, 119-127.

Fabbro, D., Ruetz, S., Buchdunger, E., Cowan-Jacob, S.W., Fendrich, G., Liebetanz, J., Mestan, J., O'Reilly, T., Traxler, P., Chaudhuri, B., Fretz, H., Zimmermann, J., Meyer, T., Carvatti, G., Furet, P., Manley, P.W. (2002). Protein kinases as targets for anticancer agents: from inhibitors to useful drugs. Pharmacology and Therapeutics, 93, 79-98.

Fairbarin, D.W., Olive, P.L., O'Neil, K.L. 1995. The comet assay: a comprehensive review. Mutation Research/Reviews in Genetic Toxicology, 339(1), 37-59.

Francisco, D.C., Peddi, Prakash, Hairr, J.M., Flood, B.A., Cecil, A.M., Kalogernis, P.T., Sigounas, G., Georgakilas, A.G. (2007). Induction and processing of complex DNA damage in human breast cancer cells MCF-7 and nonmalignant MCF-10A cells. Free Radical Biology and Medicine, 44, 558-569.

Georgakilas, A. G. (2008). Processing of DNA damage clusters in human cells: Current status of knowledge. Molecular Biosystems, 4, 30-35.

Georgakilas, A.G., Bennett, P.V., Wilson III, D.M., Sutherland, B.M. (2004). Processing of bistranded abasic DNA clusters in gamma irradiated human hematopoietic cells. Nucleic Acids Research, 32, 5609-5620.

Gollapalle, E., Eong, R., Adetolu, R., Tsao, D., Francisco, D., Sigounas, G., Georgakilas, A.G. (2007). Detection of oxidative clustered DNA lesions in X-irradiated mouse skin tissue and human MCF7 breast cancer cells. Radiation Research, 167, 207-216.

Goodhead, D.T. (1994). Initial events in the cellular effects of ionizing radiations: clustered damage in DNA. Int. Journal of Radiation. Biology, 65, 7-17.

HADA, M. and Georgakilas, A.G. (2008). Formation of clustered DNA damage after high-LET irradiation: a review. Journal of Radiation Research, 49, 203-210.

Hashimoto, M.; Donald, C. D.; Yannone, S. M.; Chen, D. J.; Roy, R.; Kow, Y. W. (2001). A possible role of Ku in mediating sequential repair of closely opposed lesions. Journal of Biological Chemistry, 276, 12827-12831.

Holt, S. M.; Georgakilas, A. G. (2007). Detection of complex DNA damage in γ-irradiated acute lymphoblastic leukemia pre-B NALM-6 cells. Radiation Research, 168, 527-534.

Hudson, J.J.R., Hsu, D., Kunde, G., Zhukovskaya, N., Liu, P., Williams, J.G., Pears, C.J., Lakin, N.D. (2005). DNA-PKcs dependent signaling of DNA damage in dictyostelium discoideum. Current Biology, 15(20), 1880-1885.

Jackson, S.P. (2002). Sensing and repairing DNA double-strand breaks. Carcinogenesis, 23(5), 687-696.

Jemal, A., Siegal, R., Ward, E., Hao, Y., Xu, J., Thun, M.J. (2009). Cancer statistics. A Cancer Journal for Clinicians, 59, 225-249.

Kashishian, A., Douangpanya, H., Clark, D., Schlachter, S.T., Early, C.T., Schiro, J.G., Huang, H., Burgess, L.E., Kesicki, E.A., Halbrook, J. (2003). DNA-Dependent protein kinase inhibitors as drug candidates for the treatment of cancer. Molecular Cancer Therapeutics, 2(12), 1257-1264.

Kastan, B.M., Bartek, J. (2004). Cell-cycle checkpoints and cancer. Nature, 432, 316-323.

Lees-Miller, S.P., Godbout, R., Chan, D.W., Weinfeld, M., Day III, R.S., Barron, G.M., Turner, J.A. 1995. Absence of p350 subunit of DNA-activated protein kinase from a radiosensitive human cell line. Science, 267, 1183-1185.

Levy, N., Martz, A., Bresson, A., Spenlehauer, C., Murcia, G., Murcia, J.M. (2006). XRCC1 is phosphorylated by DNA-dependent protein kinase in response to DNA damage. Nucleic Acids Research, 34(1), 32-41.

Lindahl, T., Wood, R.D., (1999). Quality control of DNA repair. Science, 286, 1897-1905.

Malyarchuk, S.; Castore, R.; Harrison, L. (2008). DNA repair of clustered lesions in mammalian cells: involvement of non-homologous end-joining. Nucleic Acids Research, 36, 4872-4882.

Meek, K.; Douglas, P.; Cui, X.; Ding, Q.; Lees-Miller, S. P. (2007). trans Autophosphorylation at DNA-dependent protein kinase's two major autophosphorylation site clusters facilitates end processing but not end joining. Molecular Cell Biology, 27, 3881-3890.

Meek, K.; Dang, V.; Lees-Miller, S. P.; Frederick, W. A. (2008). Chapter 2 DNA-PK: The means to justify the ends? Adv. Immunology: Academic Press, 2008, 33-58.

Miller, E. (1978). Some current perspectives on chemical carcinogens in humans in experimental animals: presidential address. Cancer Research, 38, 1479-1496.

Mourgues, S., Lomax, M.E., O'Neil, P. (2007). Base excision repair processing of abasic site/single-strand break lesions within clustered damage sites associated with XRCC1 deficiency. Nucleic Acids Research, 35(22), 7676-7687.

Nilsen, H., Krokan, H.E. (2001). Base excision repair in a network of defense and tolerance. Carcinogenesis, 22, 987-998.

Nugoli, M., Chuchana, P., Vendrell, J., Orsetti, B., Ursule, L., Nguyen, C., Birnbaum, D., Douzery, E.J.P., Cohen, P., Theillet, C. (2003). Genetic variability in MCF-7 sublines: evidence of rapid genomic and RNA expression profile modifications. Cancer, 3, 13.

O'Connor, T.R., Graves, R.J., de Murcia, G., Castaing, B., Laval, J. (1992). Fpg protein of escherichia coli is a zinc finger protein whose cysteine residues have a structural and/or functional role. The Journal of Biological Chemistry, 268(12), 9063-9070.

Parkin, D.M., Bray, F., Ferlay, J., Pisani, P. (2002). Global cancer statistics. A Cancer Journal for Clinicians, 55, 74-108.

Parlanti, E.; Locatelli, G.; Maga, G.; Dogliotti, E. (2007). Human base excision repair complex is physically associated to DNA replication and cell cycle regulatory proteins Nucleic Acids Research, 35, 1569-1577.

Parsons, D.W. et al. (2008). An integrated genomic analysis of human glioblastoma multiforme. Science, 321, 1807-1812.

Peddi, P., Francisco, D.C., Cecil, A.M., Hair, J.M., Panayoitidis, M.I., Georgakilas, A.G. (2008). Processing of clustered DNA damage in human breast cancer cells MCF-7 with partial DNA-PKcs deficiency. Cancer Letters, 269(1), 174-183.

Pouget, J.P., Felon, S., Revanat, J.L., Testard, I., Odin, F., Cadet, J. (2002). Formation of modified DNA bais in cells exposed to either gamma irradiation or to high-LET particles. Radiation Research, 157, 589-595.

Saito, Y., Uraki, F., Satoshi, N., Asaeda, A., Ono, K., Kubo, K, Yamamato, K. (1997). Characterization of endonuclease III (nth) and endonuclease VIII (nei) mutants of escherichia coli K-12. Journal of Bacteriology, 179(11), 3783-3785.

Schwartz, D.C., Cantor, C.R. (1984). Separation of yeast chromosomes-sized DNAs by pulsed field gradient gel electrophoresis. Cell, 37(1), 67-75.

Shirvastav, M., DeHaro, L.P., Nicoloff, J.A. (2008). Regualtion of DNA double strand break repair pathway choice. Cell Research, 18(1), 134-147.

Smith, G.C.M., and Jackson, S.P. (1999). The DNA-dependent protein kinase. Genes Dev., 13, 916-934.

Stupp et al, (2005). Radiotherapy plus concomitiant and adjuvant temozolomide for glioblastoma. New England Journal of Medicine, 352, 987-96.

Sutherland, B.M., Georgakilas, A.G., Bennett, P.V., Laval, J., Sutherland J.C. (2003). Quantifying clustered DNA damage induction and repair by gel electrophoresis, electronic imaging and number average length analysis. Mutation Research, 531, 93-107.

Sutherland, B.M., Bennet, P.V., Sidorkina, O., Laval, J. (2000). Clustered damages and total lesions induced in DNA by ionizing radiation: oxidized bases and strand breaks. Biochemistry, 39, 8026-8031.

Sutherland, B.M., Bennett, P.V., Sidorkina, O., Laval. J. (1999). Clustered DNA damage induced in isolated DNA and in human cells by low doses of ionizing radiation. Proceeding of the National Academy of Sciences, 97, 103-108.

Thompson, L.H., Brookman, K.W., Jones, N.J., Allen, S.A., Carrano, A.V. (1990). Molecular cloning of the human XRCC1 gene, which corrects defective DNA strand break repair and sister chromatid exchange. Molecular and Cellular Biology, 10(12), 6160-6171.

Tsao, D.; Kalogerinis, P.; Tabrizi, I.; Dingfelder, M.; Stewart, R. D.; Georgakilas, A. G. (2007). Induction and processing of clustered DNA lesions in ^{56}Fe-ion-irradiated human monocytes. Radiation Research, 168, 87-97.

Toulany, M.; Dittmann, K.; Fehrenbacher, B.; Schaller, M.; Baumann, M.; Rodemann, H. P. (2008). PI3K-Akt signaling regulates basal, but MAP-kinase signaling regulates radiation-induced XRCC1 expression in human tumor cells in vitro. DNA Repair, 7, 1746-1756.

Veuger, S. J.; Curtin, N. J.; Richardson, C. J.; Smith, G. C. M.; Durkacz, B. W. (2003). Radiosensitization and DNA repair inhibition by the combined use of novel inhibitors of DNA-dependent Protein kinase and poly(ADP-Ribose) polymerase-1. Cancer Research, 63, 6008-6015.

Visvardis, E. E.; Haveles, K. S.; Pataryas, T. A.; Margaritis, L. H.; V., S.; Sideris, E.G. (2000). Diversity of peripheral blood mononuclear cells as revealed by a novel multiple microgel "comet assay". Environmental and Molecular Mutagenesis, 36, 32-39.

Wang, S., Gong, Z., Chen, R., Liu, Y., Li, A., Li, G., and Zhou, J. (2009). JWA regulates XRCC1 and functions as a novel base excision repair protein in oxidative stress-induced DNA single-strand breaks. Nucleic Acids Research, 37(6), 1936-1950.

Ward, J.F. (1994). The complexity of DNA damage: relevance to biological consequences. Int. Journal of Radiation Biology, 66, 427-432.

Ward, J.F. (1981). Some biochemical consequences of the spatial distribution of ionizing radiation produced free radicals. Radiation Research, 86, 185-195.

Weinberg, R. (1996). How Cancer Arises. Scientific American, 275(3), 62-70.

Weinfeld, M., Rauli-Nia, A., Chaudry, M.A., Britten, R.A. (2001). Response of base excision repair enzymes to complex DNA lesions. Radiation Research, 156, 584-589.

Wilmore, E., Caux, S., Sunter, N.J., Tilby, M.J. Jackson, G.H., Austin, C.A., Durkacz, B.W. (2004). A novel DNA-dependent protein kinase inhibitor, NU7026, potentiates the cytotoxicity of topoisomerase II poisons used in the treatment of leukemia. Blood, 103(12), 4659-4665.

APPENDIX: SAFETY COMPLIANCE FORMS

The Brody School of Medicine
Office of Prospective Health
East Carolina University
188 Warren Life Sciences Building • Greenville, NC 27834
252-744-2070 office • 252-744-2417 fax

Occupational Medicine
Employee Health

March 31, 2010

Radiation Safety

Infection Control

Biological Safety

To Whom It May Concern:

Please note that Charles William Loftin, Jr. is up-to-date on his Bloodborne Pathogen and TB training. He has successfully attended and passed all Bloodborne Pathogen and TB training requirements while at ECU.

Sincerely,

Nikki Page
Office of Prospective Health
252-744-3823

Environmental Health and Safety
East Carolina University
210 East Fourth Street ~ Greenville, NC 27858-4353
252-328-6166 office ~ **252-737-1458** fax
www.ecu.edu/oehs

E A S T
CAROLINA
UNIVERSITY

Emergency Response

Environmental Management

Industrial Hygiene

Occupational Safety

Workers' Compensation

To: Charles Loftin

From: Kelly Shook, Health Sciences Coordinator
           Office of Environmental Health and Safety

Date: March 29, 2010

Subject: Chemical Hygiene/Laboratory Safety Training

Dear Mr. Loftin,

This letter is to serve as documentation that you completed the Chemical Hygiene/Laboratory Safety training as required by the Office of Environmental Health and Safety. Your attendance is on file with our office as well as on OneStop.

This training was initiated upon revision of the East Carolina University Chemical Hygiene Plan in September 2007. Topics included standard safety procedures applicable to all ECU laboratories, as well as responsibilities, chemical management and medical consultation. This training is considered current until the Fall 2010 revision and updated training program.

Please contact me with any questions or concerns.

Sincerely,

Kelly E. Shook

Kelly E. Shook, MSEH, AOES
Health Sciences Coordinator
Office of Environmental Health and Safety
East Carolina University

3/29/2010
Page 1

The Brody School of Medicine
Office of Prospective Health
East Carolina University
188 Warren Life Sciences Building ● Greenville, NC 27834
252-744-2070 office ● 252-744-2417 fax

Occupational Medicine
Employee Health

Radiation Safety

Infection Control

Biological Safety

March 30, 2010

Charles my records indicate that you attended the 6 hour basic radiation safety course on September 27, 2007.

Marcus Jeannette, MSEH
Radiation Safety Officer